

Inclusive J/ψ production at forward and backward rapidity in p-Pb collisions at $\sqrt{s_{NN}}=8.16$ TeV

Original

Inclusive J/ψ production at forward and backward rapidity in p-Pb collisions at $\sqrt{s_{NN}}=8.16$ TeV / Acharya, S.; Acosta, F. T.; Adamova, D.; Adolfsson, J.; Aggarwal, M. M.; Aglieri Rinella, G.; Agnello, M.; Bufalino, S.; Concas, M.; Grosa, F.; Ravasenga, I. - In: JOURNAL OF HIGH ENERGY PHYSICS. - ISSN 1029-8479. - STAMPA. - 2018:7(2018). [10.1007/JHEP07(2018)160]

Availability:

This version is available at: 11583/2746957 since: 2022-09-29T14:07:19Z

Publisher:

Springer Verlag

Published

DOI:10.1007/JHEP07(2018)160

Terms of use:

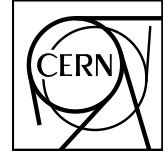
This article is made available under terms and conditions as specified in the corresponding bibliographic description in the repository

Publisher copyright

Springer postprint/Author's Accepted Manuscript

This version of the article has been accepted for publication, after peer review (when applicable) and is subject to Springer Nature's AM terms of use, but is not the Version of Record and does not reflect post-acceptance improvements, or any corrections. The Version of Record is available online at: [http://dx.doi.org/10.1007/JHEP07\(2018\)160](http://dx.doi.org/10.1007/JHEP07(2018)160)

(Article begins on next page)



CERN-EP-2018-101
10 May 2018

**Inclusive J/ψ production
at forward and backward rapidity in p–Pb collisions at $\sqrt{s_{NN}} = 8.16$ TeV**

ALICE Collaboration*

Abstract

Inclusive J/ψ production is studied in p–Pb interactions at a centre-of-mass energy per nucleon–nucleon collision $\sqrt{s_{NN}} = 8.16$ TeV, using the ALICE detector at the CERN LHC. The J/ψ meson is reconstructed, via its decay to a muon pair, in the centre-of-mass rapidity intervals $2.03 < y_{cms} < 3.53$ and $-4.46 < y_{cms} < -2.96$, where positive and negative y_{cms} refer to the p-going and Pb-going direction, respectively. The transverse momentum coverage is $p_T < 20$ GeV/ c . In this paper, y_{cms} - and p_T -differential cross sections for inclusive J/ψ production are presented, and the corresponding nuclear modification factors R_{pPb} are shown. Forward results show a suppression of the J/ψ yield with respect to pp collisions, concentrated in the region $p_T \lesssim 5$ GeV/ c . At backward rapidity no significant suppression is observed. The results are compared to previous measurements by ALICE in p–Pb collisions at $\sqrt{s_{NN}} = 5.02$ TeV and to theoretical calculations. Finally, the ratios R_{FB} between forward- and backward- y_{cms} R_{pPb} values are shown and discussed.

arXiv:1805.04381v2 [nucl-ex] 17 Jan 2019

© 2018 CERN for the benefit of the ALICE Collaboration.

Reproduction of this article or parts of it is allowed as specified in the CC-BY-4.0 license.

*See Appendix A for the list of collaboration members

1 Introduction

Quarkonium production in nuclear collisions is sensitive to the temperature of the produced medium. In particular, the various quarkonium states are expected to melt in a Quark-Gluon Plasma (QGP), due to screening of the colour interaction in a deconfined state [1]. In addition, the abundant charm-quark production in the multi-TeV collision-energy range can also lead to a (re)generation of charmonia during the QGP evolution and at the phase boundary [2, 3]. A detailed investigation of these processes was carried out by ALICE, which has measured inclusive J/ψ production in Pb–Pb collisions down to zero transverse momentum (p_{T}). These results were reported at centre-of-mass energies per nucleon pair $\sqrt{s_{\text{NN}}} = 2.76$ and 5.02 TeV, at forward centre-of-mass rapidity y_{cms} [4–7] for both energies, and at central y_{cms} for $\sqrt{s_{\text{NN}}} = 2.76$ TeV [8]. The nuclear modification factor R_{AA} was evaluated, corresponding to the ratio between the Pb–Pb and the pp production cross sections, normalised to the number of nucleon-nucleon collisions. A suppression of the J/ψ was observed, as indicated by values of R_{AA} smaller than unity. However, the suppression was found to be systematically smaller with respect to results obtained at RHIC energies [9, 10]. In addition, the suppression effects were less strong at low p_{T} . These observations, together with the comparison to theoretical model calculations [11–14] and the measurement of a non-zero elliptic flow for the J/ψ [15], imply that a fraction of the J/ψ yield is produced via recombination of charm quarks, and that recombination is more prevalent at low p_{T} , where the bulk of charm-quark production occurs.

In addition to effects connected with the hot medium, cold nuclear matter (CNM) effects are expected to influence the charmonium yield in nuclear collisions. One of the most important is nuclear shadowing, i.e., the modification of the quark and gluon structure functions for nucleons inside nuclei (see e.g., Refs. [16–18]). This effect modifies the probability for a quark or a gluon to carry a given fraction x of the momentum of the nucleon. It affects the elementary production cross section for the creation of the $c\bar{c}$ pair that will eventually form a charmonium state. Modifications of the initial state of the nucleus are also addressed by calculations incorporating parton saturation, a coherent effect involving low- x quarks and gluons, described by the Colour Glass Condensate (CGC) effective theory [19]. In addition to these mechanisms, a coherent energy-loss effect involving partons in the initial and final state can also lead to a modification of the parton kinematics and consequently to a change in the quarkonium yields with respect to elementary nucleon-nucleon collisions [20]. Finally, once produced, the charmonium state could be dissociated via inelastic interactions with the surrounding nucleons [21]. This process, which plays a dominant role among CNM effects at low collision energy [22, 23], should become negligible at the LHC, where the crossing time of the two nuclei is much shorter than the formation time of the resonance [24–26].

The CNM effects introduced above are present in nucleus-nucleus collisions, but can be more directly investigated by studying proton-nucleus collisions, where the contribution of hot-matter effects are thought to be negligible. Previous results from p–Pb collisions at $\sqrt{s_{\text{NN}}} = 5.02$ TeV from ALICE [27–29], LHCb [30] and CMS [31] have shown a significant suppression of the J/ψ yield at forward rapidity (p-going direction) and low to intermediate p_{T} ($\lesssim 5$ GeV/ c). No significant effects, or at most a slight enhancement, were seen at high p_{T} and at backward y_{cms} (Pb-going direction). The results were compared to theoretical calculations that include various combinations of all the effects mentioned in the previous paragraph, except charmonium dissociation in cold nuclear matter [32–37]. A good agreement with the models was found, indicating on the one hand that mechanisms like shadowing, CGC-related effects and coherent energy loss can account for the observed nuclear effects, and on the other hand that final state break-up processes in nuclear matter have a negligible influence. It should be noted that the model of Ref. [34] includes the effects of the interaction of charmonia with a dense hadronic medium possibly created in p–Pb collisions. However, such a medium may be expected to dissociate the weakly bound $\psi(2S)$ state [26], but should have little or no effect on the strongly bound J/ψ meson.

In 2016, p–Pb collisions at $\sqrt{s_{\text{NN}}} = 8.16$ TeV were delivered by the LHC. The interest in J/ψ stud-

ies at this energy is threefold: first, a significantly larger integrated luminosity with respect to studies performed at $\sqrt{s_{\text{NN}}} = 5.02$ TeV [27–29] has become available in ALICE, allowing a more detailed comparison to model calculations and an extended p_{T} reach. Second, by varying the collision energy, it is possible to extend the investigations of shadowing and other CNM effects to a partly different x range. Finally, studies of various physics observables in p–Pb and high-multiplicity pp collisions at the LHC have shown effects such as long-range two-particle correlations [38–43] and an enhancement of strange and multi-strange hadron production [44], already seen in Pb–Pb collisions. These effects are usually connected with the formation of an extended system of strongly interacting particles. Concerning the specific case of charmonium production, in addition to the observations discussed above, long-range correlation structures in J/ψ production were recently observed in p–Pb collisions at $\sqrt{s_{\text{NN}}} = 8.16$ TeV [45]. Furthermore, for the weakly bound $\psi(2S)$ a suppression signal, on top of the CNM effects discussed in the previous paragraphs, was seen in p–Pb and related to the resonance break-up in the medium created in such collisions [26, 46]. As mentioned above, no extra suppression needs to be introduced for the strongly bound J/ψ in order to reproduce the experimental observations at $\sqrt{s_{\text{NN}}} = 5.02$ TeV. However, higher energy p–Pb collisions may create a more extended and longer-lived medium, which might lead to a suppression effect also on the J/ψ .

In this paper, we report ALICE results on cross sections and nuclear modification factors for inclusive J/ψ production in p–Pb collisions at $\sqrt{s_{\text{NN}}} = 8.16$ TeV, in the rapidity regions $2.03 < y_{\text{cms}} < 3.53$ and $-4.46 < y_{\text{cms}} < -2.96$, and for $p_{\text{T}} < 20$ GeV/ c . In Sec. 2, the experimental apparatus, the data sample and the event selection criteria are presented. Section 3 contains a description of the analysis procedure, including a discussion of the evaluation of the systematic uncertainties. The results and their comparison to theoretical models, to recent LHCb results [47] and to $\sqrt{s_{\text{NN}}} = 5.02$ TeV data are shown in Sec. 4, while conclusions are drawn in Sec. 5.

2 Experimental apparatus, data sample and event selection

The ALICE detector design and performance are extensively described in [48, 49]. The analysis presented here is based on the detection of muons in the ALICE forward muon spectrometer [50], which includes five tracking stations (Cathode Pad Chamber detectors), followed by two triggering stations (Resistive Plate Chamber detectors). An absorber, 10 interaction-length (λ_{I}) thick and made of carbon, concrete and steel, positioned in front of the tracking system, filters out most hadrons produced in the collision. A second (7.2 λ_{I} thick) iron absorber, positioned between the tracking and the triggering system, absorbs secondary hadrons escaping the first absorber and low-momentum muons. Finally, a 3 T·m dipole magnet, positioned in the region of the third tracking station, provides the track bending for momentum evaluation. Particles are detected in the pseudo-rapidity range $-4 < \eta < -2.5$ in the laboratory system and muon triggering is performed with a programmable transverse momentum threshold, set to $p_{\mu,\text{T}} = 0.5$ GeV/ c for the data sample analysed in this paper. The trigger threshold is not sharp, and the single muon trigger efficiency reaches its plateau value ($\sim 96\%$) at $p_{\mu,\text{T}} \sim 1.5$ GeV/ c .

In addition to the muon spectrometer, four other sets of detectors play an important role for this analysis. The Silicon Pixel Detector (SPD) [51], with its two layers covering the pseudo-rapidity intervals $|\eta| < 2$ and $|\eta| < 1.4$, is part of the ALICE central barrel and is used to reconstruct the primary vertex. A coincidence of a signal in the two V0 scintillator detectors [52], covering $2.8 < \eta < 5.1$ and $-3.7 < \eta < -1.7$, provides a minimum-bias (MB) trigger. The luminosity determination is obtained from the V0 information and, independently, using the T0 Cherenkov detectors [53], which cover $4.6 < \eta < 4.9$ and $-3.3 < \eta < 3.0$. Finally, the timing information from the V0 and the Zero Degree Calorimeters (ZDC) [54] is used to remove beam-induced background.

The trigger condition used in the analysis is a $\mu\mu$ – MB trigger formed by the coincidence of the MB trigger and an unlike-sign dimuon trigger. By taking data in two configurations of the beams correspond-

ing to either protons or Pb ions going towards the muon spectrometer, it was possible to cover the dimuon rapidity ranges $2.03 < y_{\text{cms}} < 3.53$ and $-4.46 < y_{\text{cms}} < -2.96$, respectively. The two configurations are also referred to as p–Pb and Pb–p in the following.

The data samples used in this analysis correspond to an integrated luminosity $\mathcal{L}_{\text{int}}^{\text{pPb}} = 8.4 \pm 0.2 \text{ nb}^{-1}$ for p–Pb, and $\mathcal{L}_{\text{int}}^{\text{Pbp}} = 12.8 \pm 0.3 \text{ nb}^{-1}$ for Pb–p collisions [55]. These values are larger by about a factor 2 with respect to $\sqrt{s_{\text{NN}}} = 5.02$ p–Pb collision data [27].

The selection criteria used by ALICE in previous J/ψ analyses [27, 28] have been applied. Namely, both muons belonging to the pair must have $-4 < \eta_{\mu} < -2.5$, to reject tracks at the edges of the acceptance. In addition, each muon must have $17.6 < R_{\text{abs}} < 89.5$ cm, where R_{abs} is the radial transverse position of the muon tracks at the end of the absorber, to remove tracks crossing its thicker region, where energy loss and multiple scattering effects are more important. Finally, each track reconstructed in the tracking chambers of the muon spectrometer has to match a trigger track reconstructed in the trigger system.

3 Data analysis

The analysis procedure is the same for the two data sets discussed in this paper, and very similar to the one reported in Refs. [27, 28] for the $\sqrt{s_{\text{NN}}} = 5.02$ TeV p–Pb sample. The inclusive J/ψ production cross section was obtained from

$$\frac{d^2\sigma_{\text{pPb}}^{J/\psi}}{dy_{\text{cms}}dp_{\text{T}}} = \frac{N_{J/\psi}(\Delta y_{\text{cms}}, \Delta p_{\text{T}})}{\mathcal{L}_{\text{int}}^{\text{pPb}} \cdot (A \times \varepsilon)_{(\Delta y_{\text{cms}}, \Delta p_{\text{T}})} \cdot \text{B.R.}(J/\psi \rightarrow \mu^+ \mu^-) \cdot \Delta y_{\text{cms}} \cdot \Delta p_{\text{T}}} \quad (1)$$

where $N_{J/\psi}(\Delta y_{\text{cms}}, \Delta p_{\text{T}})$ is the number of reconstructed J/ψ in the $(\Delta y_{\text{cms}}, \Delta p_{\text{T}})$ interval under consideration, $(A \times \varepsilon)_{(\Delta y_{\text{cms}}, \Delta p_{\text{T}})}$ is the corresponding product of acceptance times reconstruction efficiency, $\text{B.R.}(J/\psi \rightarrow \mu^+ \mu^-) = 5.961 \pm 0.033\%$ is the branching ratio for the decay to a muon pair [56] and $\mathcal{L}_{\text{int}}^{\text{pPb}}$ is the integrated luminosity for the data sample under study.

The quantities $N_{J/\psi}(\Delta y_{\text{cms}}, \Delta p_{\text{T}})$ were obtained through fits to the invariant mass spectra of the opposite-sign muon pairs. The fitting functions are the sum of two resonance contributions (J/ψ and $\psi(2S)$) and a continuum background. For the resonances [57], an “extended” Crystal Ball (CB2) function was adopted, which accommodates a non-Gaussian tail both on the right and on the left side of the resonance peak. Alternatively, a pseudo-Gaussian function was used, corresponding to a resonance Gaussian core around the J/ψ pole and tails on the right and left side of it, parameterised by varying the width of the Gaussian as a function of the mass. The background was described by empirical functions, either with a Gaussian with a mass-dependent width or with an exponential function times a fourth-order polynomial [57]. Fits were performed using all the combinations of the signal and background functions, and varying the fitting ranges ($2.2 < m_{\mu\mu} < 4.5$ GeV/ c^2 or $2 < m_{\mu\mu} < 5$ GeV/ c^2). Figure 1 shows an example of fits to the invariant mass distributions of the p–Pb and Pb–p data samples, for opposite-sign dimuons in the region $p_{\text{T}} < 20$ GeV/ c .

When fitting the mass spectra, the value of the J/ψ mass and its width (σ) at the pole position are free parameters of the fit. The contribution of the $\psi(2S)$ was found to have a negligible impact on the evaluation of $N_{J/\psi}$.

A study of the influence of the non-Gaussian tails of the shapes of the reconstructed resonance spectra was also performed. The corresponding fit parameters were extracted either from the MC or directly from data. In the latter case, the tail parameters were evaluated either by leaving them as free parameters in the fit to the p–Pb and Pb–p samples, or using values obtained from the corresponding pp data samples at $\sqrt{s} = 8$ TeV [58] (about the same energy of the collisions under study) or $\sqrt{s} = 13$ TeV [59] (largest data sample collected by ALICE).

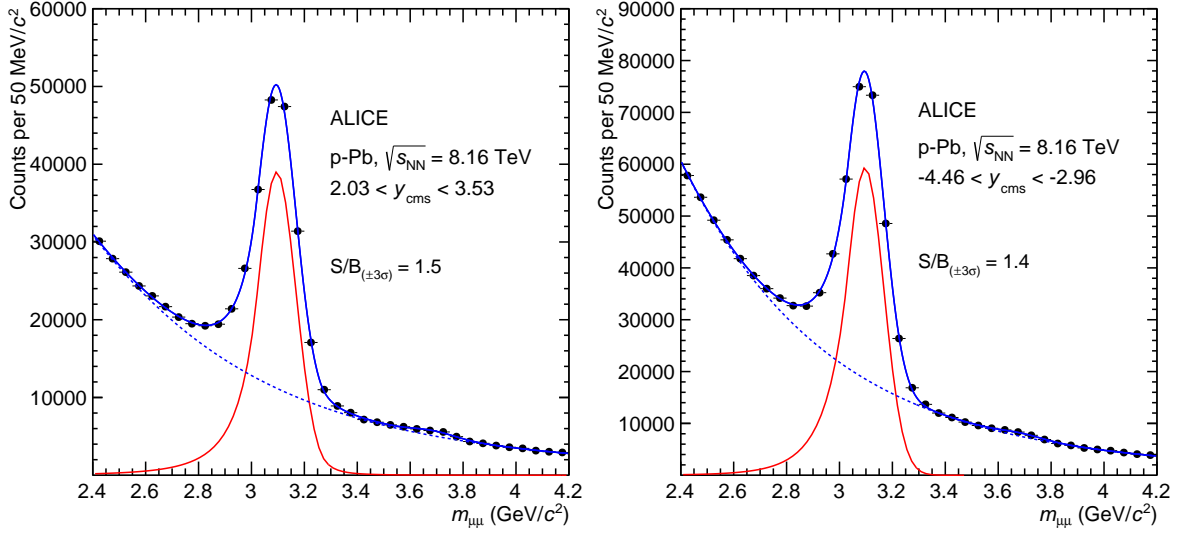


Fig. 1: Fits to the invariant mass distributions of opposite-sign dimuons with $p_T < 20$ GeV/c. The left plot refers to $2.03 < y_{\text{cms}} < 3.53$, and that on the right to $-4.46 < y_{\text{cms}} < -2.96$. The shapes of both the resonances and the background are also shown.

The $N_{J/\psi}$ values were finally obtained as the average of the results of all the fits performed. The statistical uncertainties were obtained as the average of the statistical uncertainties over the various fits, while the standard deviations of the $N_{J/\psi}$ distributions were taken as the systematic uncertainties. Typical values of the signal over background ratio in a 3σ window around the J/ψ peak range from 1.4 (0.7) to 2.8 (1.4) from low to high p_T in p–Pb (Pb–p) collisions. For the p_T -integrated data samples ($p_T < 20$ GeV/c), $N_{J/\psi}$ amounts to $(1.67 \pm 0.01 \pm 0.05) \cdot 10^5$ and $(2.52 \pm 0.01 \pm 0.08) \cdot 10^5$ for p–Pb and Pb–p respectively, where the first uncertainty is statistical and the second systematic. The latter quantity (which amounts in percentage terms to $\sim 3\%$) is dominated by the choice of the J/ψ tail parameters. When extracting $N_{J/\psi}$ in narrower p_T and y_{cms} ranges, the systematic uncertainties turn out to be similar (from 3% up to 4% in the highest p_T bins).

The quantity $(A \times \epsilon)_{(\Delta y_{\text{cms}}, \Delta p_T)}$ was evaluated by means of MC simulations, performed separately for each data taking run, in order to follow the evolution of the detector conditions. The input p_T and y_{cms} distributions for the J/ψ were tuned directly to the data by means of an iterative procedure. In detail, a first set of differential distributions, corresponding to the results of the measurements performed at $\sqrt{s_{\text{NN}}} = 5.02$ TeV [28], was taken as an input to the calculation, and the resulting $(A \times \epsilon)_{(\Delta y_{\text{cms}}, \Delta p_T)}$ values were then used to correct the raw J/ψ distributions obtained from the fits of the invariant mass spectra. The corrected differential distributions were then used as an input for another $(A \times \epsilon)_{(\Delta y_{\text{cms}}, \Delta p_T)}$ calculation, and so on. Convergence was reached at the second iteration. The p_T -integrated values of $(A \times \epsilon)$ are 0.2646 ± 0.0001 (p–Pb) and 0.2349 ± 0.0001 (Pb–p), where the quoted uncertainties are statistical.

The systematic uncertainties are related to the corresponding uncertainties on the trigger and tracking efficiencies, as well as to the choice of the input distributions. Concerning the efficiencies, for the muon trigger the procedure already used for the analysis of p–Pb data at $\sqrt{s_{\text{NN}}} = 5.02$ TeV was followed [27, 28]. The response function of the muon trigger obtained in MC and in data was used for the J/ψ $(A \times \epsilon)_{(\Delta y_{\text{cms}}, \Delta p_T)}$ calculation. Integrating over p_T , a difference of 2.4% (2.9%) on the trigger efficiency for J/ψ was estimated in p–Pb (Pb–p) collisions. The difference can become as high as 4% for low- p_T J/ψ . A 1% contribution due to the uncertainty on the intrinsic efficiency of the muon-trigger detectors was then added in quadrature to the quoted uncertainties. For the tracking efficiency, the corre-

sponding systematic uncertainty was calculated by comparing the efficiencies evaluated in data and MC. The efficiency of each tracking plane was obtained using the redundancy of the tracking system (two independent planes per station). Then, the single muon tracking efficiencies were calculated according to the tracking algorithm, and finally combined, in order to get the dimuon tracking efficiency. The estimated value of the systematic uncertainty on the tracking efficiency is 1% (2%) for p_{T} -integrated J/ψ production in p–Pb (Pb–p) collisions, and shows no appreciable dependence on the dimuon kinematics. A further systematic uncertainty, related to the choice of the χ^2 cut applied to the matching of tracks reconstructed in the muon tracking and triggering systems, was also included. Its value is 1%, independent of p_{T} and y_{cms} . Finally, the choice of the MC input distributions was found to induce a 0.5% systematic uncertainty on the acceptance calculation for the p_{T} -integrated data samples. This effect is due to the statistical uncertainty on the measured y_{cms} and p_{T} distributions that were used for the calculation, and to possible correlations between the distributions in the two kinematic variables. The maximum value of this uncertainty becomes 3% at very low p_{T} (< 1 GeV/ c).

The integrated luminosities for the two data samples were obtained from $\mathcal{L}_{\text{int}} = N_{\text{MB}}/\sigma_{\text{MB}}$ where N_{MB} is the number of MB events and σ_{MB} the cross section corresponding to the MB trigger condition. The latter quantity was evaluated from a van der Meer scan, obtaining 2.09 ± 0.03 b for p–Pb and 2.10 ± 0.04 b for Pb–p [55]. The N_{MB} quantity was estimated as $N_{\mu\mu-\text{MB}} \cdot F_{\text{norm}}$, where $N_{\mu\mu-\text{MB}}$ is the number of analysed dimuon triggers and F_{norm} is the inverse of the probability of having a triggered dimuon in a MB event. F_{norm} was calculated using the event trigger information, as the ratio between the number of collected MB triggers and the number of times the MB condition is verified together with the dimuon trigger condition, with the latter information obtained from the level-0 trigger mask. The F_{norm} values were evaluated, and corrected for the small pile-up contribution to the MB sample ($\sim 3\%$ on average), for each run and finally averaged using as a weight the number of $\mu\mu - \text{MB}$ triggers. In this way one obtains $F_{\text{norm}}^{\text{pPb}} = 679 \pm 7$ and $F_{\text{norm}}^{\text{PbPb}} = 371 \pm 4$. The quoted uncertainties (1%) are systematic and were obtained by comparing the results of the evaluation described above with an alternative method based on the information of the trigger scalers [27]. Statistical uncertainties on F_{norm} are negligible.

The nuclear effects on J/ψ production in p–Pb collisions were estimated via the nuclear modification factor, defined as:

$$R_{\text{pPb}}(y_{\text{cms}}, p_{\text{T}}) = \frac{d^2\sigma_{\text{pPb}}^{J/\psi}/dy_{\text{cms}}dp_{\text{T}}}{A_{\text{Pb}} \cdot d^2\sigma_{\text{pp}}^{J/\psi}/dy_{\text{cms}}dp_{\text{T}}} \quad (2)$$

where the p–Pb production cross section is normalised to the corresponding quantity for pp collisions times the atomic mass number of the Pb nucleus ($A_{\text{Pb}} = 208$).

The reference pp cross section was evaluated starting from the available results for forward- y_{cms} inclusive J/ψ production at $\sqrt{s} = 8$ TeV from ALICE [58] and LHCb [60]. These results are in fair agreement, as their maximum difference is 1.4σ , in the region close to $y_{\text{cms}} = 2.5$. Since the ALICE pp data cover a different y_{cms} -range ($2.5 < y_{\text{cms}} < 4$) with respect to those accessible in p–Pb and Pb–p collisions, a rapidity extrapolation by $\sim \pm 0.5$ y -units was performed to match the kinematic window of the various samples, following the procedure described in [61]. In addition, a \sqrt{s} -interpolation [59] was performed to account for the small difference in the centre-of-mass energy between pp and proton-nucleus collisions.

The rapidity extrapolation was performed on the ALICE data using three different functions (Gaussian, 2nd and 4th degree polynomials) and taking the weighted average of the extrapolated values. The associated systematic uncertainty was calculated as the maximum difference between the results obtained with the different functions. Typical values are $\sim 2 - 3\%$, reaching a maximum of $\sim 25\%$ at the very edge of the extrapolation region. For LHCb, the same procedure was used in order to match the rapidity binning of the p–Pb and Pb–p data. The procedure corresponds in this case to an interpolation, because of the

Source	p–Pb ($2.03 < y_{\text{cms}} < 3.53$)			Pb–p ($-4.46 < y_{\text{cms}} < -2.96$)		
	Integrated	vs p_{T}	vs y_{cms}	Integrated	vs p_{T}	vs y_{cms}
Signal extraction	3.1%	2.9–4.2%	3.1–3.2%	3.4%	2.7–4.0%	3.1–3.3%
MC input	0.5%	1–3%	1%	0.5%	1–2%	1–2%
Tracking efficiency	1%	1%	1%	2%	2%	2%
Trigger efficiency	2.6%	1.4–4.1%	2.2–4.1%	3.1%	1.4–4.1%	3.2–4.1%
Matching efficiency	1%	1%	1%	1%	1%	1%
$\mathcal{L}_{\text{int}}^{\text{pPb}}$ (uncorrelated)	2.1%			2.2%		
$\mathcal{L}_{\text{int}}^{\text{pPb}}$ (correlated)	0.5%			0.7%		
B.R.($J/\psi \rightarrow \mu^+ \mu^-$)	0.6%					
pp reference (unc.)	1.5%	3.5–17.0%	1.6–3.5%	1.8%	3.6–15.4%	1.8–5.9%
pp reference (corr.)	7.1%					

Table 1: Summary of systematic uncertainties on the calculation of cross sections and nuclear modification factors. Uncertainties on signal extraction, MC input and efficiencies are considered as uncorrelated over p_{T} and y_{cms} . The uncertainties on the luminosity and on the pp reference result from the combination of two contributions, one uncorrelated and the other correlated, which are separately quoted. The uncorrelated uncertainty on luminosity includes the contribution of the systematic uncertainty on F_{norm} as well as a 1.1% (0.6%) contribution due to the difference between the luminosities obtained with the V0 and T0 detectors.

larger rapidity acceptance ($2 < y_{\text{cms}} < 4.5$) of LHCb. Finally, the weighted average of the ALICE/LHCb based extrapolations/interpolations was calculated, and a small correction factor (1.5%), obtained via a \sqrt{s} -interpolation of data at various centre-of-mass energies, was introduced to account for the slight centre-of-mass energy difference between p–Pb ($\sqrt{s_{\text{NN}}} = 8.16$ TeV) and pp data ($\sqrt{s} = 8$ TeV).

For the p_{T} -differential studies, the reference pp cross section was obtained as a weighted average of the ALICE and LHCb p_{T} -differential cross sections at $\sqrt{s} = 8$ TeV [58, 60], extrapolated/interpolated to the proton-nucleus rapidity domains. The ALICE values, which are extrapolated beyond the measured pp rapidity range, were also corrected by p_{T} -dependent factors, which account for the softening/hardening of the p_{T} -differential cross section when y_{cms} increases/decreases, and were calculated from the LHCb pp results on the p_{T} -differential inclusive J/ψ cross section in narrow y_{cms} bins [60]. Since the p_{T} coverage of pp data at $\sqrt{s} = 8$ TeV by LHCb extends only up to $p_{\text{T}} = 14$ GeV/ c , a linear extrapolation of the correction factors up to $p_{\text{T}} = 20$ GeV/ c was performed. The size of this correction is $< 10\%$ for $p_{\text{T}} \lesssim 6$ GeV/ c and increases up to $\sim 40\%$ in the highest p_{T} bin. The uncertainty associated with this correction factor is small (1–2%), thanks to the very good accuracy of the LHCb results. Finally, the effect of the slight centre-of-mass energy difference between proton-nucleus and pp data sets ranges from 1% to 3.5% when increasing p_{T} .

Table 1 summarises the systematic uncertainties on the various contributions entering the cross section and the nuclear modification factor determination. The uncertainty on the integrated luminosity is the sum in quadrature of the uncertainties on σ_{MB} [55] and F_{norm} . The fractions correlated/uncorrelated between p–Pb and Pb–p measurements are separately quoted.

4 Results

In Fig. 2 the differential cross sections are presented for inclusive J/ψ production as a function of rapidity in p–Pb and Pb–p collisions, integrated over the transverse momentum interval $p_{\text{T}} < 20$ GeV/ c . The same figure shows the reference cross sections for pp collisions, obtained through the interpolation procedure described in Sec. 3 and scaled by A_{Pb} . Figure 3 reports the p–Pb differential cross sections as a function of p_{T} , separately for the forward ($2.03 < y_{\text{cms}} < 3.53$) and backward ($-4.46 < y_{\text{cms}} < -2.96$) rapidity regions, where the corresponding pp cross sections scaled by A_{Pb} are also superimposed. The comparison

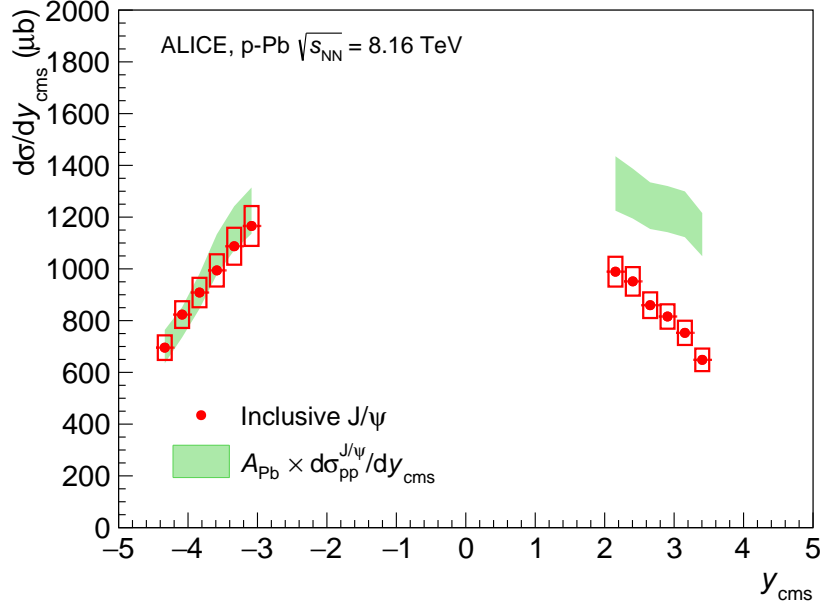


Fig. 2: The y -differential inclusive J/ψ production cross section in p–Pb and Pb–p collisions at $\sqrt{s_{\text{NN}}} = 8.16$ TeV. The vertical error bars (not visible because smaller than the symbols) represent the statistical uncertainties, the boxes around the points the systematic uncertainties. The horizontal bars correspond to the bin size. The values of the reference pp cross sections, obtained through the interpolation/extrapolation procedure described in Sec. 3, scaled by A_{Pb} , are shown as bands.

of proton-nucleus and scaled pp cross sections shows that at forward y_{cms} a suppression of the inclusive J/ψ production is visible, while no significant nuclear effects can be seen at backward y_{cms} .

Nuclear effects, already visible from the different behaviour of p–Pb and pp-scaled cross sections, are quantified through the nuclear modification factors, shown as a function of y_{cms} in Fig. 4 and of p_{T} in Fig. 5. The results are compared with the corresponding nuclear modification factors at $\sqrt{s_{\text{NN}}} = 5.02$ TeV [28]. Although the $\sqrt{s_{\text{NN}}} = 8.16$ TeV data are systematically lower, the difference is not significant given the uncertainties of the measurements. As a function of y_{cms} , R_{pPb} decreases when moving from the Pb-going to the p-going direction, showing a significant suppression at forward rapidity, while the negative rapidity measurements do not show any significant deviation from unity. As a function of p_{T} , an increase is seen at forward y_{cms} and the data become compatible with unity for $p_{\text{T}} \gtrsim 5$ GeV/ c . At negative y_{cms} an increasing trend is also likely to be present at low transverse momentum, as shown by a fit in the region $p_{\text{T}} < 4$ GeV/ c with a constant function, which gives $\chi^2/\text{ndf} = 3.3$. For $p_{\text{T}} > 4$ GeV/ c the nuclear modification factor is systematically larger than 1, but compatible with unity within 1.9σ .

Concerning the compatibility of the results at the two energies, the integration over different p_{T} ranges ($p_{\text{T}} < 8$ GeV/ c for $\sqrt{s_{\text{NN}}} = 5.02$ TeV data, $p_{\text{T}} < 20$ GeV/ c at $\sqrt{s_{\text{NN}}} = 8.16$ TeV) in Fig. 4 leads to only a small relative effect on the nuclear modification factors. In fact, when restricting the integration domain of the $\sqrt{s_{\text{NN}}} = 8.16$ TeV data to $p_{\text{T}} < 8$ GeV/ c the R_{pPb} values decrease by less than 1.5%.

The nuclear modification factors integrated over rapidity, separately in the forward and backward regions, are

$$R_{\text{pPb}}(2.03 < y_{\text{cms}} < 3.53) = 0.700 \pm 0.005(\text{stat.}) \pm 0.065(\text{syst.}) \quad (3)$$

$$R_{\text{PbP}}(-4.46 < y_{\text{cms}} < -2.96) = 1.018 \pm 0.004(\text{stat.}) \pm 0.098(\text{syst.}) \quad (4)$$

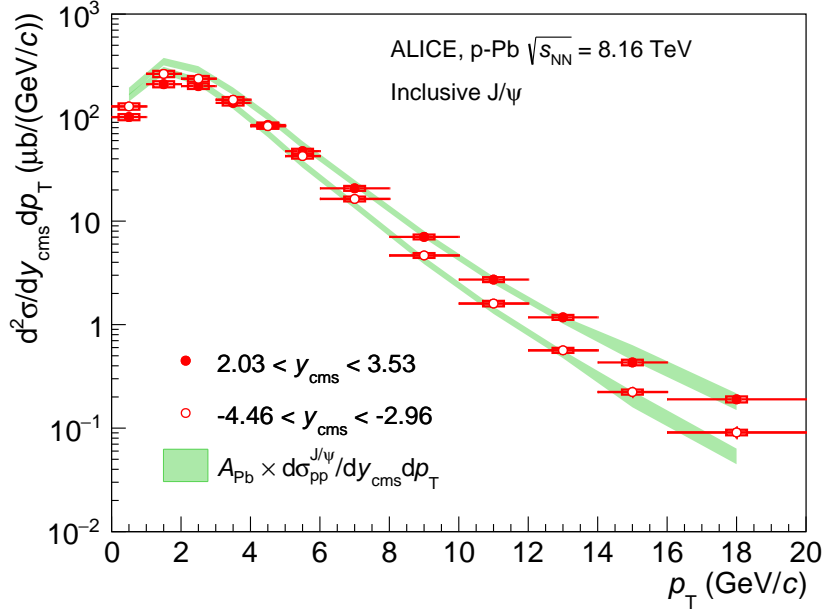


Fig. 3: The p_T -differential inclusive J/ψ production cross section in p–Pb and Pb–p collisions at $\sqrt{s_{\text{NN}}} = 8.16$ TeV. The vertical error bars (not visible because smaller than the symbols) represent the statistical uncertainties, the boxes around the points the systematic uncertainties. The horizontal bars correspond to the bin size. The values of the reference pp cross sections, obtained through the interpolation/extrapolation procedure described in Sec. 3, scaled by A_{Pb} , are shown as bands.

demonstrating that the suppression of the J/ψ production at forward rapidity in p–Pb collisions is a 4.6σ effect. The corresponding significance for the $\sqrt{s_{\text{NN}}} = 5.02$ TeV [28] data was 3.9σ . The ratios of the nuclear modification factors obtained at $\sqrt{s_{\text{NN}}} = 8.16$ and 5.02 TeV, in the region $p_T < 8$ GeV/c, are

$$R_{\text{pPb}}(8.16 \text{ TeV})/R_{\text{pPb}}(5.02 \text{ TeV})(2.03 < y_{\text{cms}} < 3.53) = 0.987 \pm 0.015(\text{stat.}) \pm 0.141(\text{syst.}) \quad (5)$$

$$R_{\text{PbPb}}(8.16 \text{ TeV})/R_{\text{PbPb}}(5.02 \text{ TeV})(-4.46 < y_{\text{cms}} < -2.96) = 0.938 \pm 0.009(\text{stat.}) \pm 0.139(\text{syst.}) \quad (6)$$

Both values are compatible with unity. The choice of the p_T range for the calculation of the ratios is related to the maximum reach of the $\sqrt{s_{\text{NN}}} = 5.02$ TeV results.

In Fig. 6 the ALICE results are compared to the corresponding LHCb values [47], which cover a slightly wider y_{cms} range and are integrated up to $p_T = 14$ GeV/c, showing a good agreement between the two measurements. The LHCb results refer to prompt J/ψ production, i.e., include decays of higher-mass charmonium states but do not include the contribution from b-hadron decays (non-prompt production). For the region $p_T \leq 5$ GeV/c, which dominates the p_T -integrated results, the size of the latter contribution amounts to 10–15% of the inclusive production. An estimate of the difference between prompt and inclusive nuclear modification factors, based on LHCb results [47], gives a 3–4% (1–2%) effect at positive (negative) y_{cms} .

In Fig. 6 a comparison with the results of several theoretical models for prompt J/ψ production is also presented. The results of two calculations based on a pure shadowing scenario (Vogt [62], Lansberg et al. [37, 63]) show good agreement with data when the nCTEQ15 [17] or EPPS16 [18] set of nuclear parton distribution functions (nPDF) is adopted, while using the EPS09 [16] set of nPDF leads to a slightly worse agreement at forward y_{cms} . Calculations based on a CGC approach coupled with various elementary production models are able to reproduce the data in their domain of validity, corresponding to the

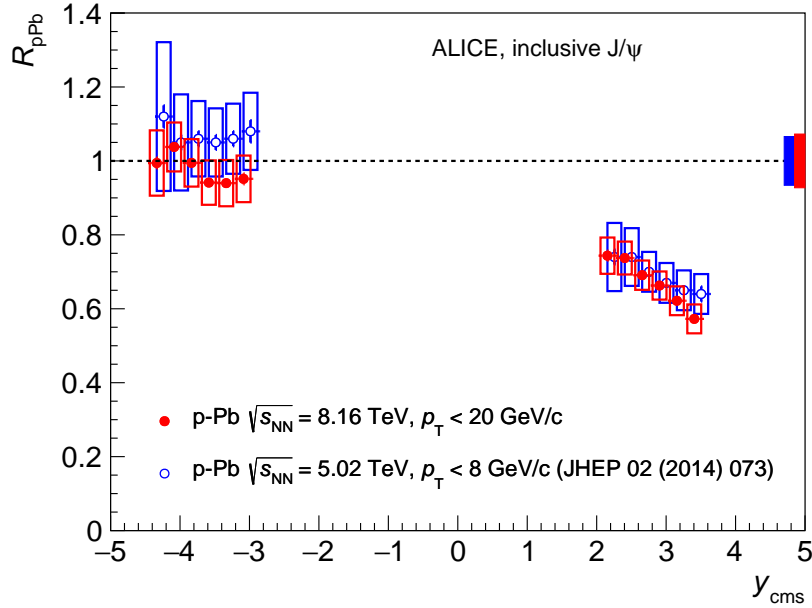


Fig. 4: The inclusive J/ψ nuclear modification factor in p–Pb and Pb–p collisions at $\sqrt{s_{\text{NN}}} = 8.16$ TeV, as a function of y_{cms} . The horizontal bars correspond to the bin size. The vertical error bars represent the statistical uncertainties, the boxes around the points the uncorrelated systematic uncertainties. Correlated uncertainties are shown as a filled box around unity for each energy. The results are compared with those for p–Pb and Pb–p collisions at $\sqrt{s_{\text{NN}}} = 5.02$ TeV [28]. The latter have been plotted at slightly shifted y_{cms} values, for better visibility.

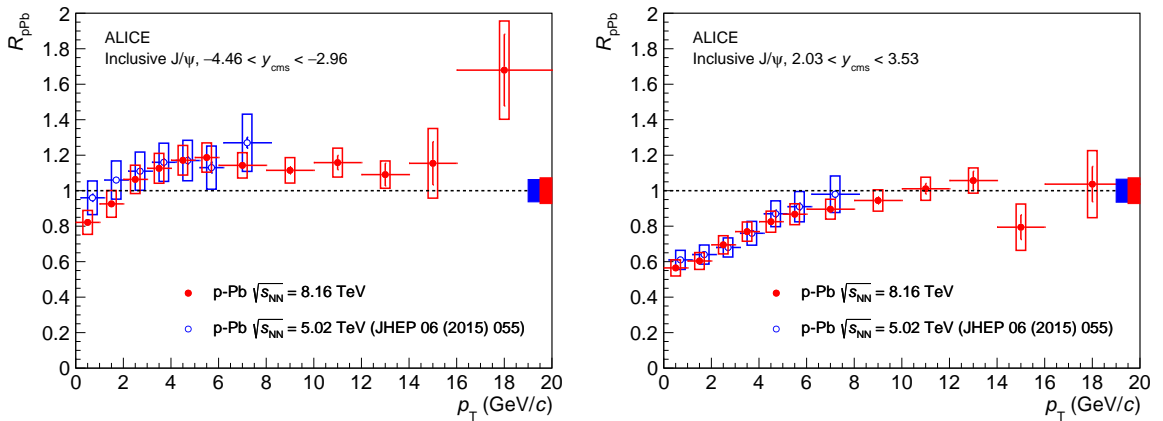


Fig. 5: The inclusive J/ψ nuclear modification factor in Pb–p (left) and p–Pb (right) collisions at $\sqrt{s_{\text{NN}}} = 8.16$ TeV, as a function of p_{T} . The horizontal bars correspond to the bin size. The vertical error bars represent the statistical uncertainties, the boxes around the points the uncorrelated systematic uncertainties. Correlated uncertainties are shown as a filled box around unity for each energy. The results are compared with those for p–Pb and Pb–p collisions at $\sqrt{s_{\text{NN}}} = 5.02$ TeV [28]. The latter have been plotted at a slightly shifted p_{T} , for better visibility.

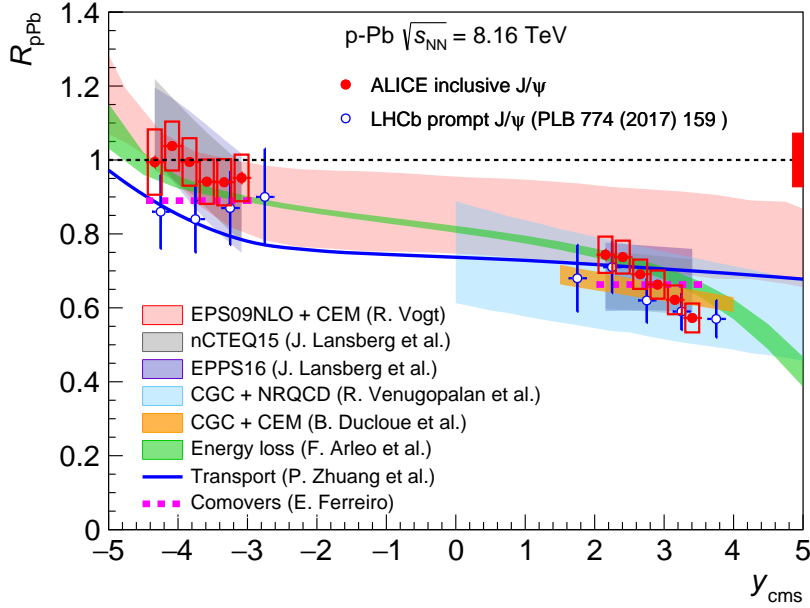


Fig. 6: Comparison of the ALICE and LHCb [47] results on the y_{cms} -dependence of the J/ψ nuclear modification factors in p–Pb and Pb–p collisions at $\sqrt{s_{\text{NN}}} = 8.16$ TeV. The horizontal bars correspond to the bin size. For ALICE, the vertical error bars represent the statistical uncertainties, the boxes around the points the uncorrelated systematic uncertainties, and the filled box around unity the correlated uncertainties. For LHCb, the vertical error bars represent the combination of statistical and systematic uncertainties. The results are also compared to several model calculations [34, 37, 62, 64–67] (see text for details).

forward- y_{cms} region (Venugopalan et al. [64], Ducloue et al. [65]). The model of Arleo et al. [66], based on the calculation of the effects of parton coherent energy loss, gives a good description of backward- y_{cms} results and reproduces the data at forward y_{cms} fairly well. Finally, models including a contribution from the final state interaction of the $c\bar{c}$ pair with the partonic/hadronic system created in the collision (Ferreiro [34], Zhuang et al. [67]) can also reproduce the trend observed in the data. In such a class of models nuclear shadowing is included, and is anyway the process that plays a dominant role in determining the values of the nuclear modification factors.

Figure 7 shows a comparison of the p_{T} -dependence of R_{pPb} and R_{PbPb} with the calculations of the models discussed above. Thanks to the extended p_{T} range, these data explore a wide x interval. At $y_{\text{cms}} = 2.78$ (centre of the forward- y interval), the covered range for $0 < p_{\text{T}} < 20$ GeV/ c is $2.3 \cdot 10^{-5} < x < 1.5 \cdot 10^{-4}$ while at $y_{\text{cms}} = -3.71$ one has $1.5 \cdot 10^{-2} < x < 10^{-1}$. These values were calculated in the so-called $2 \rightarrow 1$ approach, where the production channel is based on the gluon fusion process $gg \rightarrow J/\psi$. The agreement between data and models is rather good. It should be noted that for models that include uncertainty bands, such uncertainties are generally larger than those of the data, both as a function of y_{cms} and p_{T} .

By forming the ratio of the nuclear modification factors at forward and backward rapidity, it is possible to obtain a quantity, R_{FB} , with smaller uncertainties, provided that the same absolute values of the y_{cms} -ranges are chosen for the ratio. In this way, the reference pp cross section, and the related uncertainties, cancel out. R_{FB} is calculated in the rapidity range $2.96 < |y_{\text{cms}}| < 3.53$, which is covered by both p–Pb and Pb–p samples. In Fig. 8 the y_{cms} - and p_{T} -dependence of R_{FB} are shown, and compared with the corresponding results at $\sqrt{s_{\text{NN}}} = 5.02$ TeV [27]. No appreciable dependence on y_{cms} can be seen, while R_{FB} steadily increases as a function of p_{T} , reaching unity at $p_{\text{T}} \sim 12$ GeV/ c . Results at $\sqrt{s_{\text{NN}}} = 8.16$ and 5.02 TeV are compatible within uncertainties.

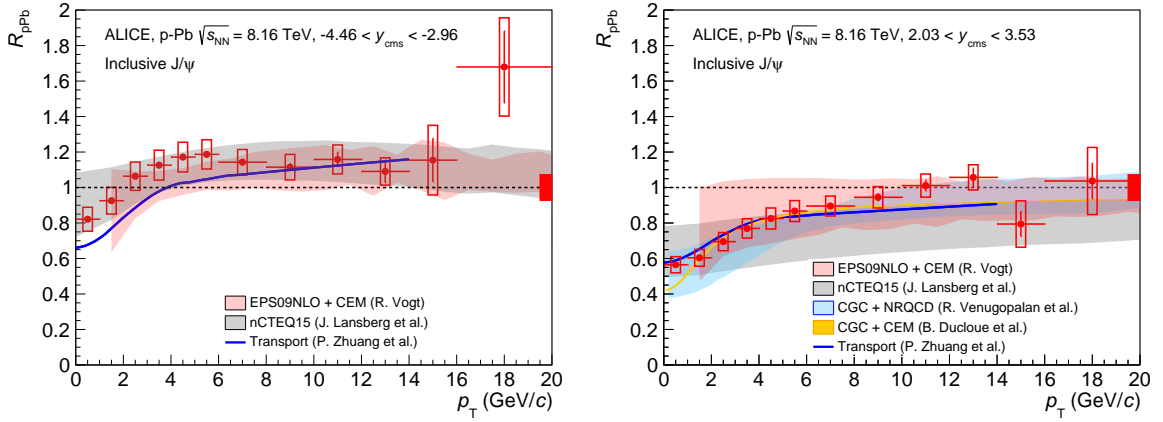


Fig. 7: Comparison of the ALICE results on the p_T -dependence of the inclusive J/ψ nuclear modification factors in Pb–p (left) and p–Pb (right) collisions at $\sqrt{s_{NN}} = 8.16$ TeV with model calculations [34, 37, 62, 64–67] (see text for details). The horizontal bars on the experimental points correspond to the bin size. The vertical error bars represent the statistical uncertainties, the boxes around the points the uncorrelated systematic uncertainties and the filled box around unity the correlated uncertainties.

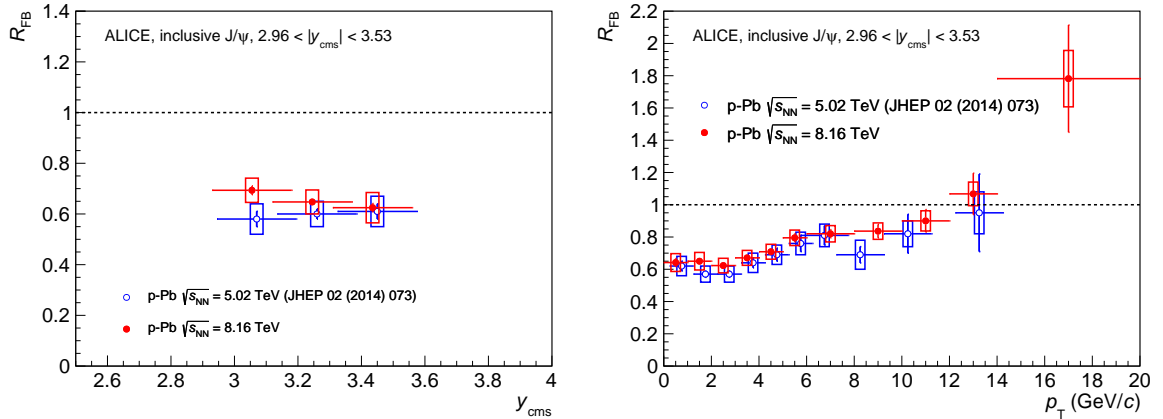


Fig. 8: The ratio R_{FB} between the inclusive J/ψ nuclear modification factors, as a function of y_{cms} (left) and p_T (right), relative to $2.96 < |y_{cms}| < 3.53$. The horizontal bars correspond to the bin size. The vertical error bars represent the statistical uncertainties, the boxes around the points the systematic uncertainties. The results are compared with those obtained at $\sqrt{s_{NN}} = 5.02$ TeV [27]. The latter have been plotted at a slightly shifted y_{cms} and p_T , for better visibility.

5 Conclusions

Inclusive J/ψ production in p–Pb collisions at $\sqrt{s_{\text{NN}}} = 8.16$ TeV was measured by ALICE, with about twice the integrated luminosity of the corresponding data sample at $\sqrt{s_{\text{NN}}} = 5.02$ TeV [28]. Results on the cross sections and on the nuclear modification factors were shown, in six rapidity bins, for the p-going ($2.03 < y_{\text{cms}} < 3.53$) and Pb-going ($-4.46 < y_{\text{cms}} < -2.96$) directions. The corresponding results as a function of transverse momentum were also shown, separately for the two y_{cms} regions, for $p_{\text{T}} < 20$ GeV/ c . A suppression of the J/ψ was observed at positive y_{cms} , concentrated in the $p_{\text{T}} \lesssim 5$ GeV/ c range. For negative y_{cms} , an increasing trend in the nuclear modification factor is present at low p_{T} , and the data are compatible with unity within 1.9σ for $p_{\text{T}} > 4$ GeV/ c . The ratios R_{FB} between forward- and backward- y_{cms} R_{pPb} in the region $2.96 < |y_{\text{cms}}| < 3.53$ were also shown as a function of y_{cms} and p_{T} . The results on the nuclear modification factors and on R_{FB} were found to be compatible with those obtained at $\sqrt{s_{\text{NN}}} = 5.02$ TeV. A good agreement is also observed when comparing ALICE and LHCb results at $\sqrt{s_{\text{NN}}} = 8.16$ TeV. Finally, a comparison with several theory predictions shows that the results can be reproduced fairly well by calculations including various combinations of cold nuclear matter effects.

Acknowledgements

The ALICE Collaboration would like to thank all its engineers and technicians for their invaluable contributions to the construction of the experiment and the CERN accelerator teams for the outstanding performance of the LHC complex. The ALICE Collaboration gratefully acknowledges the resources and support provided by all Grid centres and the Worldwide LHC Computing Grid (WLCG) collaboration. The ALICE Collaboration acknowledges the following funding agencies for their support in building and running the ALICE detector: A. I. Alikhanyan National Science Laboratory (Yerevan Physics Institute) Foundation (ANSL), State Committee of Science and World Federation of Scientists (WFS), Armenia; Austrian Academy of Sciences and Nationalstiftung für Forschung, Technologie und Entwicklung, Austria; Ministry of Communications and High Technologies, National Nuclear Research Center, Azerbaijan; Conselho Nacional de Desenvolvimento Científico e Tecnológico (CNPq), Universidade Federal do Rio Grande do Sul (UFRGS), Financiadora de Estudos e Projetos (Finep) and Fundação de Amparo à Pesquisa do Estado de São Paulo (FAPESP), Brazil; Ministry of Science & Technology of China (MSTC), National Natural Science Foundation of China (NSFC) and Ministry of Education of China (MOEC), China; Ministry of Science and Education, Croatia; Ministry of Education, Youth and Sports of the Czech Republic, Czech Republic; The Danish Council for Independent Research — Natural Sciences, the Carlsberg Foundation and Danish National Research Foundation (DNRF), Denmark; Helsinki Institute of Physics (HIP), Finland; Commissariat à l’Energie Atomique (CEA) and Institut National de Physique Nucléaire et de Physique des Particules (IN2P3) and Centre National de la Recherche Scientifique (CNRS), France; Bundesministerium für Bildung, Wissenschaft, Forschung und Technologie (BMBF) and GSI Helmholtzzentrum für Schwerionenforschung GmbH, Germany; General Secretariat for Research and Technology, Ministry of Education, Research and Religions, Greece; National Research, Development and Innovation Office, Hungary; Department of Atomic Energy Government of India (DAE), Department of Science and Technology, Government of India (DST), University Grants Commission, Government of India (UGC) and Council of Scientific and Industrial Research (CSIR), India; Indonesian Institute of Science, Indonesia; Centro Fermi - Museo Storico della Fisica e Centro Studi e Ricerche Enrico Fermi and Istituto Nazionale di Fisica Nucleare (INFN), Italy; Institute for Innovative Science and Technology, Nagasaki Institute of Applied Science (IIST), Japan Society for the Promotion of Science (JSPS) KAKENHI and Japanese Ministry of Education, Culture, Sports, Science and Technology (MEXT), Japan; Consejo Nacional de Ciencia (CONACYT) y Tecnología, through Fondo de Cooperación Internacional en Ciencia y Tecnología (FONCICYT) and Dirección General de Asuntos del Personal Académico (DGAPA), Mexico; Nederlandse Organisatie voor Wetenschappelijk Onderzoek (NWO), Netherlands; The Research Council of Norway, Norway; Commission on Science and Technol-

ogy for Sustainable Development in the South (COMSATS), Pakistan; Pontificia Universidad Católica del Perú, Peru; Ministry of Science and Higher Education and National Science Centre, Poland; Korea Institute of Science and Technology Information and National Research Foundation of Korea (NRF), Republic of Korea; Ministry of Education and Scientific Research, Institute of Atomic Physics and Romanian National Agency for Science, Technology and Innovation, Romania; Joint Institute for Nuclear Research (JINR), Ministry of Education and Science of the Russian Federation and National Research Centre Kurchatov Institute, Russia; Ministry of Education, Science, Research and Sport of the Slovak Republic, Slovakia; National Research Foundation of South Africa, South Africa; Centro de Aplicaciones Tecnológicas y Desarrollo Nuclear (CEADEN), Cubaenergía, Cuba and Centro de Investigaciones Energéticas, Medioambientales y Tecnológicas (CIEMAT), Spain; Swedish Research Council (VR) and Knut & Alice Wallenberg Foundation (KAW), Sweden; European Organization for Nuclear Research, Switzerland; National Science and Technology Development Agency (NSDTA), Suranaree University of Technology (SUT) and Office of the Higher Education Commission under NRU project of Thailand, Thailand; Turkish Atomic Energy Agency (TAEK), Turkey; National Academy of Sciences of Ukraine, Ukraine; Science and Technology Facilities Council (STFC), United Kingdom; National Science Foundation of the United States of America (NSF) and United States Department of Energy, Office of Nuclear Physics (DOE NP), United States of America.

References

- [1] T. Matsui and H. Satz, “ J/ψ Suppression by Quark-Gluon Plasma Formation,” *Phys. Lett.* **B178** (1986) 416.
- [2] P. Braun-Munzinger and J. Stachel, “(Non)thermal aspects of charmonium production and a new look at J/ψ suppression,” *Phys. Lett.* **B490** (2000) 196–202.
- [3] R. L. Thews, M. Schroedter, and J. Rafelski, “Enhanced J/ψ production in deconfined quark matter,” *Phys. Rev.* **C63** (2001) 054905, arXiv:hep-ph/0007323 [hep-ph].
- [4] ALICE Collaboration, B. Abelev *et al.*, “ J/ψ suppression at forward rapidity in Pb-Pb collisions at $\sqrt{s_{NN}} = 2.76$ TeV,” *Phys. Rev. Lett.* **109** (2012) 072301, arXiv:1202.1383 [hep-ex].
- [5] ALICE Collaboration, B. Abelev *et al.*, “Centrality, rapidity and transverse momentum dependence of J/Ψ suppression in Pb-Pb collisions at $\sqrt{s_{NN}}=2.76$ TeV,” *Phys. Lett.* **B743** (2014) 314–327, arXiv:1311.0214 [nucl-ex].
- [6] ALICE Collaboration, J. Adam *et al.*, “Differential studies of inclusive J/ψ and $\psi(2S)$ production at forward rapidity in Pb-Pb collisions at $\sqrt{s_{NN}} = 2.76$ TeV,” *JHEP* **05** (2016) 179, arXiv:1506.08804 [nucl-ex].
- [7] ALICE Collaboration, J. Adam *et al.*, “ J/ψ suppression at forward rapidity in Pb-Pb collisions at $\sqrt{s_{NN}} = 5.02$ TeV,” *Phys. Lett.* **B766** (2017) 212–224, arXiv:1606.08197 [nucl-ex].
- [8] ALICE Collaboration, J. Adam *et al.*, “Inclusive, prompt and non-prompt J/ψ production at mid-rapidity in Pb-Pb collisions at $\sqrt{s_{NN}} = 2.76$ TeV,” *JHEP* **07** (2015) 051, arXiv:1504.07151 [nucl-ex].
- [9] PHENIX Collaboration, A. Adare *et al.*, “ J/ψ suppression at forward rapidity in Au+Au collisions at $\sqrt{s_{NN}} = 200$ GeV,” *Phys. Rev.* **C84** (2011) 054912, arXiv:1103.6269 [nucl-ex].
- [10] STAR Collaboration, L. Adamczyk *et al.*, “Energy dependence of J/ψ production in Au+Au collisions at $\sqrt{s_{NN}} = 39, 62.4$ and 200 GeV,” *Phys. Lett.* **B771** (2017) 13–20, arXiv:1607.07517 [hep-ex].

- [11] X. Zhao and R. Rapp, “Medium Modifications and Production of Charmonia at LHC,” *Nucl. Phys.* **A859** (2011) 114–125, arXiv:1102.2194 [hep-ph].
- [12] K. Zhou, N. Xu, Z. Xu, and P. Zhuang, “Medium effects on charmonium production at ultrarelativistic energies available at the CERN Large Hadron Collider,” *Phys. Rev.* **C89** no. 5, (2014) 054911, arXiv:1401.5845 [nucl-th].
- [13] A. Andronic, P. Braun-Munzinger, K. Redlich, and J. Stachel, “The statistical model in Pb-Pb collisions at the LHC,” *Nucl. Phys.* **A904-905** (2013) 535c–538c, arXiv:1210.7724 [nucl-th].
- [14] E. G. Ferreira, “Charmonium dissociation and recombination at LHC: Revisiting comovers,” *Phys. Lett.* **B731** (2014) 57–63, arXiv:1210.3209 [hep-ph].
- [15] ALICE Collaboration, S. Acharya *et al.*, “ J/ψ elliptic flow in Pb-Pb collisions at $\sqrt{s_{NN}} = 5.02$ TeV,” *Phys. Rev. Lett.* **119** no. 24, (2017) 242301, arXiv:1709.05260 [nucl-ex].
- [16] K. J. Eskola, H. Paukkunen, and C. A. Salgado, “EPS09: A New Generation of NLO and LO Nuclear Parton Distribution Functions,” *JHEP* **0904** (2009) 065, arXiv:0902.4154 [hep-ph].
- [17] K. Kovarik *et al.*, “nCTEQ15 - Global analysis of nuclear parton distributions with uncertainties in the CTEQ framework,” *Phys. Rev.* **D93** no. 8, (2016) 085037, arXiv:1509.00792 [hep-ph].
- [18] K. J. Eskola, P. Paakkinen, H. Paukkunen, and C. A. Salgado, “EPPS16: Nuclear parton distributions with LHC data,” *Eur. Phys. J.* **C77** no. 3, (2017) 163, arXiv:1612.05741 [hep-ph].
- [19] E. Iancu and R. Venugopalan, “The Color glass condensate and high-energy scattering in QCD,” in *Hwa, R.C. (ed.) et al.: Quark gluon plasma 249-3363*. 2003. arXiv:hep-ph/0303204 [hep-ph].
- [20] F. Arleo and S. Peigne, “Heavy-quarkonium suppression in p-A collisions from parton energy loss in cold QCD matter,” *JHEP* **1303** (2013) 122, arXiv:1212.0434 [hep-ph].
- [21] C. Gerschel and J. Hufner, “A Contribution to the Suppression of the J/ψ Meson Produced in High-Energy Nucleus Nucleus Collisions,” *Phys. Lett.* **B207** (1988) 253–256.
- [22] NA50 Collaboration, B. Alessandro *et al.*, “Charmonia and Drell-Yan production in proton-nucleus collisions at the CERN SPS,” *Phys. Lett.* **B553** (2003) 167–178.
- [23] PHENIX Collaboration, A. Adare *et al.*, “Transverse-Momentum Dependence of the J/ψ Nuclear Modification in $d+Au$ Collisions at $\sqrt{s_{NN}} = 200$ GeV,” *Phys. Rev.* **C87** no. 3, (2013) 034904, arXiv:1204.0777 [nucl-ex].
- [24] J. Hufner, Yu. P. Ivanov, B. Z. Kopeliovich, and A. V. Tarasov, “Photoproduction of charmonia and total charmonium proton cross-sections,” *Phys. Rev.* **D62** (2000) 094022, arXiv:hep-ph/0007111 [hep-ph].
- [25] D. Kharzeev and R. L. Thews, “Quarkonium formation time in a model independent approach,” *Phys. Rev.* **C60** (1999) 041901, arXiv:nucl-th/9907021 [nucl-th].
- [26] ALICE Collaboration, J. Adam *et al.*, “Centrality dependence of $\psi(2S)$ suppression in p-Pb collisions at $\sqrt{s_{NN}} = 5.02$ TeV,” *JHEP* **06** (2016) 050, arXiv:1603.02816 [nucl-ex].
- [27] ALICE Collaboration, B. Abelev *et al.*, “ J/ψ production and nuclear effects in p-Pb collisions at $\sqrt{s_{NN}} = 5.02$ TeV,” *JHEP* **1402** (2014) 073, arXiv:1308.6726 [nucl-ex].

- [28] **ALICE** Collaboration, J. Adam *et al.*, “Rapidity and transverse-momentum dependence of the inclusive J/ψ nuclear modification factor in p-Pb collisions at $\sqrt{s_{NN}} = 5.02$ TeV,” *JHEP* **06** (2015) 055, arXiv:1503.07179 [nucl-ex].
- [29] **ALICE** Collaboration, J. Adam *et al.*, “Centrality dependence of inclusive J/ψ production in p-Pb collisions at $\sqrt{s_{NN}} = 5.02$ TeV,” *JHEP* **11** (2015) 127, arXiv:1506.08808 [nucl-ex].
- [30] **LHCb** Collaboration, R. Aaij *et al.*, “Study of J/ψ production and cold nuclear matter effects in pPb collisions at $\sqrt{s_{NN}} = 5$ TeV,” *JHEP* **02** (2014) 072, arXiv:1308.6729 [nucl-ex].
- [31] **CMS** Collaboration, A. M. Sirunyan *et al.*, “Measurement of prompt and nonprompt J/ψ production in pp and pPb collisions at $\sqrt{s_{NN}} = 5.02$ TeV,” *Eur. Phys. J.* **C77** no. 4, (2017) 269, arXiv:1702.01462 [nucl-ex].
- [32] J. Albacete, N. Armesto, R. Baier, G. Barnafoldi, J. Barrette, *et al.*, “Predictions for $p+Pb$ Collisions at $\sqrt{s_{NN}} = 5$ TeV,” *Int. J. Mod. Phys.* **E22** (2013) 1330007, arXiv:1301.3395 [hep-ph].
- [33] F. Arleo, R. Kolevatov, S. Peign, and M. Rustamova, “Centrality and p_T dependence of J/ψ suppression in proton-nucleus collisions from parton energy loss,” *JHEP* **05** (2013) 155, arXiv:1304.0901 [hep-ph].
- [34] E. G. Ferreira, “Excited charmonium suppression in proton-nucleus collisions as a consequence of comovers,” *Phys. Lett.* **B749** (2015) 98–103, arXiv:1411.0549 [hep-ph].
- [35] Y.-Q. Ma, R. Venugopalan, and H.-F. Zhang, “ J/ψ production and suppression in high energy proton-nucleus collisions,” *Phys. Rev.* **D92** (2015) 071901, arXiv:1503.07772 [hep-ph].
- [36] B. Ducloue, T. Lappi, and H. Mantysaari, “Forward J/ψ production in proton-nucleus collisions at high energy,” *Phys. Rev.* **D91** no. 11, (2015) 114005, arXiv:1503.02789 [hep-ph].
- [37] J.-P. Lansberg and H.-S. Shao, “Towards an automated tool to evaluate the impact of the nuclear modification of the gluon density on quarkonium, D and B meson production in proton-nucleus collisions,” *Eur. Phys. J.* **C77** no. 1, (2017) 1, arXiv:1610.05382 [hep-ph].
- [38] **CMS** Collaboration, V. Khachatryan *et al.*, “Evidence for collectivity in pp collisions at the LHC,” *Phys. Lett.* **B765** (2017) 193–220, arXiv:1606.06198 [nucl-ex].
- [39] **CMS** Collaboration, S. Chatrchyan *et al.*, “Observation of long-range near-side angular correlations in proton-lead collisions at the LHC,” *Phys. Lett.* **B718** (2013) 795–814, arXiv:1210.5482 [nucl-ex].
- [40] **ATLAS** Collaboration, G. Aad *et al.*, “Observation of Long-Range Elliptic Azimuthal Anisotropies in $\sqrt{s} = 13$ and 2.76 TeV pp Collisions with the ATLAS Detector,” *Phys. Rev. Lett.* **116** no. 17, (2016) 172301, arXiv:1509.04776 [hep-ex].
- [41] **ATLAS** Collaboration, G. Aad *et al.*, “Observation of Associated Near-Side and Away-Side Long-Range Correlations in $\sqrt{s_{NN}}=5.02$ TeV Proton-Lead Collisions with the ATLAS Detector,” *Phys. Rev. Lett.* **110** no. 18, (2013) 182302, arXiv:1212.5198 [hep-ex].
- [42] **ALICE** Collaboration, B. Abelev *et al.*, “Long-range angular correlations on the near and away side in p -Pb collisions at $\sqrt{s_{NN}} = 5.02$ TeV,” *Phys. Lett.* **B719** (2013) 29–41, arXiv:1212.2001 [nucl-ex].

- [43] **ALICE** Collaboration, B. Abelev *et al.*, “Long-range angular correlations of π , K and p in p-Pb collisions at $\sqrt{s_{NN}} = 5.02$ TeV,” *Phys. Lett.* **B726** (2013) 164–177, arXiv:1307.3237 [nucl-ex].
- [44] **ALICE** Collaboration, J. Adam *et al.*, “Enhanced production of multi-strange hadrons in high-multiplicity proton-proton collisions,” *Nature Phys.* **13** (2017) 535–539, arXiv:1606.07424 [nucl-ex].
- [45] **ALICE** Collaboration, S. Acharya *et al.*, “Search for collectivity with azimuthal J/ψ -hadron correlations in high multiplicity p-Pb collisions at $\sqrt{s_{NN}} = 5.02$ and 8.16 TeV,” *Phys. Lett.* **B780** (2018) 7–20, arXiv:1709.06807 [nucl-ex].
- [46] **ALICE** Collaboration, B. Abelev *et al.*, “Suppression of $\psi(2S)$ production in p-Pb collisions at $\sqrt{s_{NN}} = 5.02$ TeV,” *JHEP* **12** (2014) 073, arXiv:1405.3796 [nucl-ex].
- [47] **LHCb** Collaboration, R. Aaij *et al.*, “Prompt and nonprompt J/ψ production and nuclear modification in pPb collisions at $\sqrt{s_{NN}} = 8.16$ TeV,” *Phys. Lett.* **B774** (2017) 159–178, arXiv:1706.07122 [hep-ex].
- [48] **ALICE** Collaboration, K. Aamodt *et al.*, “The ALICE experiment at the CERN LHC,” *JINST* **3** (2008) S08002.
- [49] **ALICE** Collaboration, B. Abelev *et al.*, “Performance of the ALICE Experiment at the CERN LHC,” *Int. J. Mod. Phys.* **A29** (2014) 1430044, arXiv:1402.4476 [nucl-ex].
- [50] **ALICE** Collaboration, K. Aamodt *et al.*, “Rapidity and transverse momentum dependence of inclusive J/ψ production in pp collisions at $\sqrt{s} = 7$ TeV,” *Phys. Lett.* **B704** (2011) 442–455, arXiv:1105.0380 [hep-ex].
- [51] **ALICE** Collaboration, K. Aamodt *et al.*, “Alignment of the ALICE Inner Tracking System with cosmic-ray tracks,” *JINST* **5** (2010) P03003, arXiv:1001.0502 [physics.ins-det].
- [52] **ALICE** Collaboration, E. Abbas *et al.*, “Performance of the ALICE VZERO system,” *JINST* **8** (2013) P10016, arXiv:1306.3130 [nucl-ex].
- [53] M. Bondila *et al.*, “ALICE T0 detector,” *IEEE Trans. Nucl. Sci.* **52** (2005) 1705–1711.
- [54] **ALICE** Collaboration, B. Abelev *et al.*, “Measurement of the Cross Section for Electromagnetic Dissociation with Neutron Emission in Pb-Pb Collisions at $\sqrt{s_{NN}} = 2.76$ TeV,” *Phys. Rev. Lett.* **109** (2012) 252302, arXiv:1203.2436 [nucl-ex].
- [55] **ALICE** Collaboration, “ALICE luminosity determination for p-Pb and Pb-p collisions at $\sqrt{s_{NN}} = 8.16$ TeV,” <http://cds.cern.ch/record/2314660>.
- [56] **Particle Data Group** Collaboration, C. Patrignani *et al.*, “Review of Particle Physics,” *Chin. Phys.* **C40** no. 10, (2016) 100001.
- [57] **ALICE** Collaboration, “Quarkonium signal extraction in ALICE,” *ALICE-PUBLIC-2015-006* (2015).
- [58] **ALICE** Collaboration, J. Adam *et al.*, “Inclusive quarkonium production at forward rapidity in pp collisions at $\sqrt{s} = 8$ TeV,” *Eur. Phys. J.* **C76** no. 4, (2016) 184, arXiv:1509.08258 [hep-ex].
- [59] **ALICE** Collaboration, S. Acharya *et al.*, “Energy dependence of forward-rapidity J/ψ and $\psi(2S)$ production in pp collisions at the LHC,” *Eur. Phys. J.* **C77** no. 6, (2017) 392, arXiv:1702.00557 [hep-ex].

- [60] **LHCb** Collaboration, R. Aaij *et al.*, “Production of J/ψ and Υ mesons in pp collisions at $\sqrt{s} = 8$ TeV,” *JHEP* **1306** (2013) 064, arXiv:1304.6977 [hep-ex].
- [61] **ALICE, LHCb** Collaboration, “Reference pp cross-sections for J/ψ studies in proton-lead collisions at $\sqrt{s_{NN}} = 5.02$ TeV and comparisons between ALICE and LHCb results,” <http://cds.cern.ch/record/1639617>. CONF-2013-013.
- [62] J. L. Albacete *et al.*, “Predictions for p +Pb Collisions at $\sqrt{s_{NN}} = 8.16$ TeV,” arXiv:1707.09973 [hep-ph].
- [63] A. Kusina, J.-P. Lansberg, I. Schienbein, and H.-S. Shao, “Gluon shadowing and antishadowing in heavy-flavor production at the LHC,” arXiv:1712.07024 [hep-ph].
- [64] Y.-Q. Ma, R. Venugopalan, K. Watanabe, and H.-F. Zhang, “ $\psi(2S)$ versus J/ψ suppression in proton-nucleus collisions from factorization violating soft color exchanges,” *Phys. Rev.* **C97** no. 1, (2018) 014909, arXiv:1707.07266 [hep-ph].
- [65] B. Ducloue, T. Lappi, and H. Mantysaari, “Forward J/ψ production at high energy: centrality dependence and mean transverse momentum,” *Phys. Rev.* **D94** no. 7, (2016) 074031, arXiv:1605.05680 [hep-ph].
- [66] F. Arleo and S. Peign, “Quarkonium suppression in heavy-ion collisions from coherent energy loss in cold nuclear matter,” *JHEP* **10** (2014) 073, arXiv:1407.5054 [hep-ph].
- [67] B. Chen, T. Guo, Y. Liu, and P. Zhuang, “Cold and Hot Nuclear Matter Effects on Charmonium Production in p+Pb Collisions at LHC Energy,” *Phys. Lett.* **B765** (2017) 323–327, arXiv:1607.07927 [nucl-th].

A The ALICE Collaboration

S. Acharya¹³⁸, F.T.-. Acosta²², D. Adamová⁹⁴, J. Adolfsson⁸¹, M.M. Aggarwal⁹⁸, G. Aglieri Rinella³⁶, M. Agnello³³, N. Agrawal⁴⁹, Z. Ahammed¹³⁸, S.U. Ahn⁷⁷, S. Aiola¹⁴³, A. Akindinov⁶⁵, M. Al-Turany¹⁰⁴, S.N. Alam¹³⁸, D.S.D. Albuquerque¹²⁰, D. Aleksandrov⁸⁸, B. Alessandro⁵⁹, R. Alfaro Molina⁷³, Y. Ali¹⁶, A. Alici^{11, 54, 29}, A. Alkin³, J. Alme²⁴, T. Alt⁷⁰, L. Altenkamper²⁴, I. Altsybeev¹³⁷, C. Andrei⁴⁸, D. Andreou³⁶, H.A. Andrews¹⁰⁸, A. Andronic^{141, 104}, M. Angeletti³⁶, V. Anguelov¹⁰², C. Anson¹⁷, T. Antičić¹⁰⁵, F. Antinori⁵⁷, P. Antonioli⁵⁴, R. Anwar¹²⁴, N. Apadula⁸⁰, L. Aphecetche¹¹², H. Appelshäuser⁷⁰, S. Arcelli²⁹, R. Arnaldi⁵⁹, O.W. Arnold^{103, 115}, I.C. Arsene²³, M. Arslandok¹⁰², B. Audurier¹¹², A. Augustinus³⁶, R. Averbeck¹⁰⁴, M.D. Azmi¹⁸, A. Badalá⁵⁶, Y.W. Baek^{61, 42}, S. Bagnasco⁵⁹, R. Bailhache⁷⁰, R. Bala⁹⁹, A. Baldisseri¹³⁴, M. Ball⁴⁴, R.C. Baral⁸⁶, A.M. Barbano²⁸, R. Barbera³⁰, F. Barile⁵³, L. Barioglio²⁸, G.G. Barnaföldi¹⁴², L.S. Barnby⁹³, V. Barret¹³¹, P. Bartalini⁷, K. Barth³⁶, E. Bartsch⁷⁰, N. Bastid¹³¹, S. Basu¹⁴⁰, G. Batigne¹¹², B. Batyunya⁷⁶, P.C. Batzing²³, J.L. Bazo Alba¹⁰⁹, I.G. Bearden⁸⁹, H. Beck¹⁰², C. Bedda⁶⁴, N.K. Behera⁶¹, I. Belikov¹³³, F. Bellini³⁶, H. Bello Martinez², R. Bellwied¹²⁴, L.G.E. Beltran¹¹⁸, V. Belyaev⁹², G. Bencedi¹⁴², S. Beole²⁸, A. Bercuci⁴⁸, Y. Berdnikov⁹⁶, D. Berenyi¹⁴², R.A. Bertens¹²⁷, D. Berzano^{36, 59}, L. Betev³⁶, P.P. Bhaduri¹³⁸, A. Bhasin⁹⁹, I.R. Bhat⁹⁹, H. Bhatt⁴⁹, B. Bhattacharjee⁴³, J. Bhum¹¹⁶, A. Bianchi²⁸, L. Bianchi¹²⁴, N. Bianchi⁵², J. Bielčák³⁹, J. Bielčiková⁹⁴, A. Bilandzic^{115, 103}, G. Biro¹⁴², R. Biswas⁴, S. Biswas⁴, J.T. Blair¹¹⁷, D. Blau⁸⁸, C. Blume⁷⁰, G. Boca¹³⁵, F. Bock³⁶, A. Bogdanov⁹², L. Boldizsár¹⁴², M. Bombara⁴⁰, G. Bonomi¹³⁶, M. Bonora³⁶, H. Borel¹³⁴, A. Borissov^{20, 141}, M. Borri¹²⁶, E. Botta²⁸, C. Bourjau⁸⁹, L. Bratrud⁷⁰, P. Braun-Munzinger¹⁰⁴, M. Bregant¹¹⁹, T.A. Broker⁷⁰, M. Broz³⁹, E.J. Brucken⁴⁵, E. Bruna⁵⁹, G.E. Bruno^{36, 35}, D. Budnikov¹⁰⁶, H. Buesching⁷⁰, S. Bufalino³³, P. Buhler¹¹¹, P. Buncic³⁶, O. Busch^{130, i}, Z. Buthelezi⁷⁴, J.B. Butt¹⁶, J.T. Buxton¹⁹, J. Cabala¹¹⁴, D. Caffarri⁹⁰, H. Caines¹⁴³, A. Caliva¹⁰⁴, E. Calvo Villar¹⁰⁹, R.S. Camacho², P. Camerini²⁷, A.A. Capon¹¹¹, F. Carena³⁶, W. Carena³⁶, F. Carnesecchi^{29, 11}, J. Castillo Castellanos¹³⁴, A.J. Castro¹²⁷, E.A.R. Casula⁵⁵, C. Ceballos Sanchez⁹, S. Chandra¹³⁸, B. Chang¹²⁵, W. Chang⁷, S. Chapeland³⁶, M. Chartier¹²⁶, S. Chattopadhyay¹³⁸, S. Chattopadhyay¹⁰⁷, A. Chauvin^{103, 115}, C. Cheshkov¹³², B. Cheynis¹³², V. Chibante Barroso³⁶, D.D. Chinellato¹²⁰, S. Cho⁶¹, P. Chochula³⁶, T. Chowdhury¹³¹, P. Christakoglou⁹⁰, C.H. Christensen⁸⁹, P. Christiansen⁸¹, T. Chujo¹³⁰, S.U. Chung²⁰, C. Cicalo⁵⁵, L. Cifarelli^{11, 29}, F. Cindolo⁵⁴, J. Cleymans¹²³, F. Colamaria⁵³, D. Colella^{66, 36, 53}, A. Collu⁸⁰, M. Colocci²⁹, M. Concas^{59, ii}, G. Conesa Balbastre⁷⁹, Z. Conesa del Valle⁶², J.G. Contreras³⁹, T.M. Cormier⁹⁵, Y. Corrales Morales⁵⁹, P. Cortese³⁴, M.R. Cosentino¹²¹, F. Costa³⁶, S. Costanza¹³⁵, J. Crkovská⁶², P. Crochet¹³¹, E. Cuautle⁷¹, L. Cunqueiro^{141, 95}, T. Dahms^{103, 115}, A. Dainese⁵⁷, S. Dani⁶⁷, M.C. Danisch¹⁰², A. Danu⁶⁹, D. Das¹⁰⁷, I. Das¹⁰⁷, S. Das⁴, A. Dash⁸⁶, S. Dash⁴⁹, S. De⁵⁰, A. De Caro³², G. de Cataldo⁵³, C. de Conti¹¹⁹, J. de Cuveland⁴¹, A. De Falco²⁶, D. De Gruttola^{11, 32}, N. De Marco⁵⁹, S. De Pasquale³², R.D. De Souza¹²⁰, H.F. Degenhardt¹¹⁹, A. Deisting^{104, 102}, A. Deloff⁸⁵, S. Delsanto²⁸, C. Deplano⁹⁰, P. Dhankher⁴⁹, D. Di Bari³⁵, A. Di Mauro³⁶, B. Di Ruzza⁵⁷, R.A. Diaz⁹, T. Dietel¹²³, P. Dillenseger⁷⁰, Y. Ding⁷, R. Diviá³⁶, Ø. Djuvsland²⁴, A. Dobrin³⁶, D. Domenicis Gimenez¹¹⁹, B. Dönigus⁷⁰, O. Dordic²³, L.V.R. Doremalen⁶⁴, A.K. Dubey¹³⁸, A. Dubla¹⁰⁴, L. Ducroux¹³², S. Dudi⁹⁸, A.K. Duggal⁹⁸, M. Dukhishyam⁸⁶, P. Dupieux¹³¹, R.J. Ehlers¹⁴³, D. Elia⁵³, E. Endress¹⁰⁹, H. Engel⁷⁵, E. Eppe¹⁴³, B. Erazmus¹¹², F. Erhardt⁹⁷, M.R. Ersdal²⁴, B. Espagnon⁶², G. Eulisse³⁶, J. Eum²⁰, D. Evans¹⁰⁸, S. Evdokimov⁹¹, L. Fabbietti^{103, 115}, M. Faggin³¹, J. Faivre⁷⁹, A. Fantoni⁵², M. Fasel⁹⁵, L. Feldkamp¹⁴¹, A. Feliciello⁵⁹, G. Feofilov¹³⁷, A. Fernández Téllez², A. Ferretti²⁸, A. Festanti^{31, 36}, V.J.G. Feuillard¹⁰², J. Figiel¹¹⁶, M.A.S. Figueredo¹¹⁹, S. Filchagin¹⁰⁶, D. Finogeev⁶³, F.M. Fionda²⁴, G. Fiorenza⁵³, F. Flor¹²⁴, M. Floris³⁶, S. Foertsch⁷⁴, P. Foka¹⁰⁴, S. Fokin⁸⁸, E. Fragiaco⁶⁰, A. Francescon³⁶, A. Francisco¹¹², U. Frankenfeld¹⁰⁴, G.G. Fronze²⁸, U. Fuchs³⁶, C. Furget⁷⁹, A. Furs⁶³, M. Fusco Girard³², J.J. Gaardhøje⁸⁹, M. Gagliardi²⁸, A.M. Gago¹⁰⁹, K. Gajdosova⁸⁹, M. Gallio²⁸, C.D. Galvan¹¹⁸, P. Ganoti⁸⁴, C. Garabatos¹⁰⁴, E. Garcia-Solis¹², K. Garg³⁰, C. Gargiulo³⁶, P. Gasik^{115, 103}, E.F. Gauger¹¹⁷, M.B. Gay Ducati⁷², M. Germain¹¹², J. Ghosh¹⁰⁷, P. Ghosh¹³⁸, S.K. Ghosh⁴, P. Gianotti⁵², P. Giubellino^{104, 59}, P. Giubilato³¹, P. Glässel¹⁰², D.M. Gómez Coral⁷³, A. Gomez Ramirez⁷⁵, V. Gonzalez¹⁰⁴, P. González-Zamora², S. Gorbunov⁴¹, L. Görlich¹¹⁶, S. Gotovac³⁷, V. Grabski⁷³, L.K. Graczykowski¹³⁹, K.L. Graham¹⁰⁸, L. Greiner⁸⁰, A. Grelli⁶⁴, C. Grigoras³⁶, V. Grigoriev⁹², A. Grigoryan¹, S. Grigoryan⁷⁶, J.M. Gronefeld¹⁰⁴, F. Grosa³³, J.F. Grosse-Oetringhaus³⁶, R. Grosso¹⁰⁴, R. Guernane⁷⁹, B. Guerzoni²⁹, M. Guittiere¹¹², K. Gulbrandsen⁸⁹, T. Gunji¹²⁹, A. Gupta⁹⁹, R. Gupta⁹⁹, I.B. Guzman², R. Haake³⁶, M.K. Habib¹⁰⁴, C. Hadjidakis⁶², H. Hamagaki⁸², G. Hamar¹⁴², M. Hamid⁷, J.C. Hamon¹³³, R. Hannigan¹¹⁷, M.R. Haque⁶⁴, J.W. Harris¹⁴³, A. Harton¹², H. Hassan⁷⁹, D. Hatzifotiadou^{54, 11}, S. Hayashi¹²⁹, S.T. Heckel⁷⁰, E. Hellbär⁷⁰, H. Helstrup³⁸, A. Herghelegiu⁴⁸, E.G. Hernandez², G. Herrera Corral¹⁰, F. Herrmann¹⁴¹, K.F. Hetland³⁸, T.E. Hilden⁴⁵, H. Hillemanns³⁶, C. Hills¹²⁶, B. Hippolyte¹³³, B. Hohlweger¹⁰³, D. Horak³⁹, S. Hornung¹⁰⁴, R. Hosokawa^{130, 79}, J. Hota⁶⁷, P. Hristov³⁶, C. Huang⁶², C. Hughes¹²⁷, P. Huhn⁷⁰,

T.J. Humanic¹⁹, H. Hushnud¹⁰⁷, N. Hussain⁴³, T. Hussain¹⁸, D. Hutter⁴¹, D.S. Hwang²¹, J.P. Iddon¹²⁶, S.A. Iga Buitron⁷¹, R. Ilkaev¹⁰⁶, M. Inaba¹³⁰, M. Ippolitov⁸⁸, M.S. Islam¹⁰⁷, M. Ivanov¹⁰⁴, V. Ivanov⁹⁶, V. Izucheev⁹¹, B. Jacak⁸⁰, N. Jacazio²⁹, P.M. Jacobs⁸⁰, M.B. Jadhav⁴⁹, S. Jadlovska¹¹⁴, J. Jadlovsky¹¹⁴, S. Jaelani⁶⁴, C. Jahnke^{119,115}, M.J. Jakubowska¹³⁹, M.A. Janik¹³⁹, C. Jena⁸⁶, M. Jercic⁹⁷, R.T. Jimenez Bustamante¹⁰⁴, M. Jin¹²⁴, P.G. Jones¹⁰⁸, A. Jusko¹⁰⁸, P. Kalinak⁶⁶, A. Kalweit³⁶, J.H. Kang¹⁴⁴, V. Kaplin⁹², S. Kar⁷, A. Karasu Uysal⁷⁸, O. Karavichev⁶³, T. Karavicheva⁶³, P. Karczmarczyk³⁶, E. Karpechev⁶³, U. Keschull⁷⁵, R. Keidel⁴⁷, D.L.D. Keijdener⁶⁴, M. Keil³⁶, B. Ketzer⁴⁴, Z. Khabanova⁹⁰, A.M. Khan⁷, S. Khan¹⁸, S.A. Khan¹³⁸, A. Khanzadeev⁹⁶, Y. Kharlov⁹¹, A. Khatun¹⁸, A. Khuntia⁵⁰, M.M. Kielbowicz¹¹⁶, B. Kileng³⁸, B. Kim¹³⁰, D. Kim¹⁴⁴, D.J. Kim¹²⁵, E.J. Kim¹⁴, H. Kim¹⁴⁴, J.S. Kim⁴², J. Kim¹⁰², M. Kim^{61,102}, S. Kim²¹, T. Kim¹⁴⁴, T. Kim¹⁴⁴, S. Kirsch⁴¹, I. Kisel⁴¹, S. Kiselev⁶⁵, A. Kisiel¹³⁹, J.L. Klay⁶, C. Klein⁷⁰, J. Klein^{36,59}, C. Klein-Bösing¹⁴¹, S. Klewin¹⁰², A. Kluge³⁶, M.L. Knichel³⁶, A.G. Knospe¹²⁴, C. Kobdaj¹¹³, M. Kofarago¹⁴², M.K. Köhler¹⁰², T. Kollegger¹⁰⁴, N. Kondratyeva⁹², E. Kondratyuk⁹¹, A. Konevskikh⁶³, M. Konyushikhin¹⁴⁰, O. Kovalenko⁸⁵, V. Kovalenko¹³⁷, M. Kowalski¹¹⁶, I. Králik⁶⁶, A. Kravčáková⁴⁰, L. Kreis¹⁰⁴, M. Krivda^{66,108}, F. Krizek⁹⁴, M. Krüger⁷⁰, E. Kryshen⁹⁶, M. Krzewicki⁴¹, A.M. Kubera¹⁹, V. Kučera^{94,61}, C. Kuhn¹³³, P.G. Kuijper⁹⁰, J. Kumar⁴⁹, L. Kumar⁹⁸, S. Kumar⁴⁹, S. Kundu⁸⁶, P. Kurashvili⁸⁵, A. Kurepin⁶³, A.B. Kurepin⁶³, A. Kuryakin¹⁰⁶, S. Kuschpil⁹⁴, M.J. Kweon⁶¹, Y. Kwon¹⁴⁴, S.L. La Pointe⁴¹, P. La Rocca³⁰, Y.S. Lai⁸⁰, I. Lakomov³⁶, R. Langoy¹²², K. Lapidus¹⁴³, C. Lara⁷⁵, A. Lardeux²³, P. Larionov⁵², E. Laudi³⁶, R. Lavicka³⁹, R. Lea²⁷, L. Leardini¹⁰², S. Lee¹⁴⁴, F. Lehas⁹⁰, S. Lehner¹¹¹, J. Lehrbach⁴¹, R.C. Lemmon⁹³, I. León Monzón¹¹⁸, P. Lévai¹⁴², X. Li¹³, X.L. Li⁷, J. Lien¹²², R. Lietava¹⁰⁸, B. Lim²⁰, S. Lindal²³, V. Lindenstruth⁴¹, S.W. Lindsay¹²⁶, C. Lippmann¹⁰⁴, M.A. Lisa¹⁹, V. Litichevskiy⁴⁵, A. Liu⁸⁰, H.M. Ljunggren⁸¹, W.J. Llope¹⁴⁰, D.F. Lodato⁶⁴, V. Loginov⁹², C. Loizides^{95,80}, P. Loncar³⁷, X. Lopez¹³¹, E. López Torres⁹, A. Lowe¹⁴², P. Luetig⁷⁰, J.R. Luhder¹⁴¹, M. Lunardon³¹, G. Luparello⁶⁰, M. Lupi³⁶, A. Maevskaya⁶³, M. Mager³⁶, S.M. Mahmood²³, A. Maire¹³³, R.D. Majka¹⁴³, M. Malaev⁹⁶, Q.W. Malik²³, L. Malinina^{76,iii}, D. Mal'Kevich⁶⁵, P. Malzacher¹⁰⁴, A. Mamonov¹⁰⁶, V. Manko⁸⁸, F. Manso¹³¹, V. Manzari⁵³, Y. Mao⁷, M. Marchisone^{74,128,132}, J. Mareš⁶⁸, G.V. Margagliotti²⁷, A. Margotti⁵⁴, J. Margutti⁶⁴, A. Marín¹⁰⁴, C. Markert¹¹⁷, M. Marquard⁷⁰, N.A. Martin¹⁰⁴, P. Martinengo³⁶, J.L. Martinez¹²⁴, M.I. Martínez², G. Martínez García¹¹², M. Martinez Pedreira³⁶, S. Masciocchi¹⁰⁴, M. Maserà²⁸, A. Masoni⁵⁵, L. Massacrier⁶², E. Masson¹¹², A. Mastroserio⁵³, A.M. Mathis^{103,115}, P.F.T. Matuoka¹¹⁹, A. Matyja^{127,116}, C. Mayer¹¹⁶, M. Mazzilli³⁵, M.A. Mazzoni⁵⁸, F. Meddi²⁵, Y. Melikyan⁹², A. Menchaca-Rocha⁷³, E. Meninno³², J. Mercado Pérez¹⁰², M. Meres¹⁵, C.S. Meza¹⁰⁹, S. Mhlanga¹²³, Y. Miake¹³⁰, L. Micheletti²⁸, M.M. Mieskolainen⁴⁵, D.L. Mihaylov¹⁰³, K. Mikhaylov^{65,76}, A. Mischke⁶⁴, A.N. Mishra⁷¹, D. Miśkowiec¹⁰⁴, J. Mitra¹³⁸, C.M. Mitu⁶⁹, N. Mohammadi³⁶, A.P. Mohanty⁶⁴, B. Mohanty⁸⁶, M. Mohisin Khan^{18,iv}, D.A. Moreira De Godoy¹⁴¹, L.A.P. Moreno², S. Moretto³¹, A. Morreale¹¹², A. Morsch³⁶, V. Muccifora⁵², E. Mudnic³⁷, D. Mühlheim¹⁴¹, S. Muhuri¹³⁸, M. Mukherjee⁴, J.D. Mulligan¹⁴³, M.G. Munhoz¹¹⁹, K. Mürning⁴⁴, M.I.A. Muñoz⁸⁰, R.H. Munzer⁷⁰, H. Murakami¹²⁹, S. Murray⁷⁴, L. Musa³⁶, J. Musinsky⁶⁶, C.J. Myers¹²⁴, J.W. Myrcha¹³⁹, B. Naik⁴⁹, R. Nair⁸⁵, B.K. Nandi⁴⁹, R. Nania^{54,11}, E. Nappi⁵³, A. Narayan⁴⁹, M.U. Naru¹⁶, A.F. Nassirpour⁸¹, H. Natal da Luz¹¹⁹, C. Natrass¹²⁷, S.R. Navarro², K. Nayak⁸⁶, R. Nayak⁴⁹, T.K. Nayak¹³⁸, S. Nazarenko¹⁰⁶, R.A. Negrão De Oliveira^{70,36}, L. Nellen⁷¹, S.V. Nesbo³⁸, G. Neskovic⁴¹, F. Ng¹²⁴, M. Nicassio¹⁰⁴, J. Niedziela^{139,36}, B.S. Nielsen⁸⁹, S. Nikolaev⁸⁸, S. Nikulin⁸⁸, V. Nikulin⁹⁶, F. Noferini^{11,54}, P. Nomokonov⁷⁶, G. Nooren⁶⁴, J.C.C. Noris², J. Norman⁷⁹, A. Nyanin⁸⁸, J. Nystrand²⁴, H. Oh¹⁴⁴, A. Ohlson¹⁰², J. Oleniacz¹³⁹, A.C. Oliveira Da Silva¹¹⁹, M.H. Oliver¹⁴³, J. Onderwaater¹⁰⁴, C. Oppedisano⁵⁹, R. Orava⁴⁵, M. Oravec¹¹⁴, A. Ortiz Velasquez⁷¹, A. Oskarsson⁸¹, J. Otwinowski¹¹⁶, K. Oyama⁸², Y. Pachmayer¹⁰², V. Pacik⁸⁹, D. Pagano¹³⁶, G. Paic⁷¹, P. Palni⁷, J. Pan¹⁴⁰, A.K. Pandey⁴⁹, S. Panebianco¹³⁴, V. Papikyan¹, P. Pareek⁵⁰, J. Park⁶¹, J.E. Parkkila¹²⁵, S. Parmar⁹⁸, A. Passfeld¹⁴¹, S.P. Pathak¹²⁴, R.N. Patra¹³⁸, B. Paul⁵⁹, H. Pei⁷, T. Peitzmann⁶⁴, X. Peng⁷, L.G. Pereira⁷², H. Pereira Da Costa¹³⁴, D. Peresunko⁸⁸, E. Perez Lezama⁷⁰, V. Peskov⁷⁰, Y. Pestov⁵, V. Petráček³⁹, M. Petrovici⁴⁸, C. Petta³⁰, R.P. Pezzi⁷², S. Piano⁶⁰, M. Pikna¹⁵, P. Pillot¹¹², L.O.D.L. Pimentel⁸⁹, O. Pinazza^{54,36}, L. Pinsky¹²⁴, S. Pisano⁵², D.B. Piyarathna¹²⁴, M. Płoskoń⁸⁰, M. Planinic⁹⁷, F. Pliquett⁷⁰, J. Pluta¹³⁹, S. Pochybova¹⁴², P.L.M. Podesta-Lerma¹¹⁸, M.G. Poghosyan⁹⁵, B. Polichtchouk⁹¹, N. Poljak⁹⁷, W. Poonsawat¹¹³, A. Pop⁴⁸, H. Poppenborg¹⁴¹, S. Porteboeuf-Houssais¹³¹, V. Pozdniakov⁷⁶, S.K. Prasad⁴, R. Preghenella⁵⁴, F. Prino⁵⁹, C.A. Pruneau¹⁴⁰, I. Pshenichnov⁶³, M. Puccio²⁸, V. Punin¹⁰⁶, J. Putschke¹⁴⁰, S. Raha⁴, S. Rajput⁹⁹, J. Rak¹²⁵, A. Rakotozafindrabe¹³⁴, L. Ramello³⁴, F. Rami¹³³, R. Raniwala¹⁰⁰, S. Raniwala¹⁰⁰, S.S. Räsänen⁴⁵, B.T. Rascanu⁷⁰, V. Ratza⁴⁴, I. Ravasenga³³, K.F. Read^{127,95}, K. Redlich^{85,v}, A. Rehman²⁴, P. Reichelt⁷⁰, F. Reidt³⁶, X. Ren⁷, R. Renfordt⁷⁰, A. Reshetin⁶³, J.-P. Revol¹¹, K. Reygers¹⁰², V. Riabov⁹⁶, T. Richert^{64,81}, M. Richter²³, P. Riedler³⁶, W. Riegler³⁶, F. Riggi³⁰, C. Ristea⁶⁹, S.P. Rode⁵⁰, M. Rodríguez Cahuantzi², K. Røed²³, R. Rogalev⁹¹, E. Rogochaya⁷⁶, D. Rohr³⁶, D. Röhrich²⁴, P.S. Rokita¹³⁹,

F. Ronchetti⁵², E.D. Rosas⁷¹, K. Roslon¹³⁹, P. Rosnet¹³¹, A. Rossi³¹, A. Rotondi¹³⁵, F. Roukoutakis⁸⁴, C. Roy¹³³, P. Roy¹⁰⁷, O.V. Rueda⁷¹, R. Rui²⁷, B. Rumyantsev⁷⁶, A. Rustamov⁸⁷, E. Ryabinkin⁸⁸, Y. Ryabov⁹⁶, A. Rybicki¹¹⁶, S. Saarinén⁴⁵, S. Sadhu¹³⁸, S. Sadovsky⁹¹, K. Šafařík³⁶, S.K. Saha¹³⁸, B. Sahoo⁴⁹, P. Sahoo⁵⁰, R. Sahoo⁵⁰, S. Sahoo⁶⁷, P.K. Sahu⁶⁷, J. Saini¹³⁸, S. Sakai¹³⁰, M.A. Saleh¹⁴⁰, S. Sambyal⁹⁹, V. Samsonov^{96,92}, A. Sandoval⁷³, A. Sarkar⁷⁴, D. Sarkar¹³⁸, N. Sarkar¹³⁸, P. Sarma⁴³, M.H.P. Sas⁶⁴, E. Scapparone⁵⁴, F. Scarlassara³¹, B. Schaefer⁹⁵, H.S. Scheid⁷⁰, C. Schiaua⁴⁸, R. Schicker¹⁰², C. Schmidt¹⁰⁴, H.R. Schmidt¹⁰¹, M.O. Schmidt¹⁰², M. Schmidt¹⁰¹, N.V. Schmidt^{95,70}, J. Schukraft³⁶, Y. Schutz^{36,133}, K. Schwarz¹⁰⁴, K. Schweda¹⁰⁴, G. Scioli²⁹, E. Scomparin⁵⁹, M. Šefčík⁴⁰, J.E. Seger¹⁷, Y. Sekiguchi¹²⁹, D. Sekihata⁴⁶, I. Selyuzhenkov^{104,92}, K. Senosi⁷⁴, S. Senyukov¹³³, E. Serradilla⁷³, P. Sett⁴⁹, A. Sevcenco⁶⁹, A. Shabanov⁶³, A. Shabetai¹¹², R. Shahoyan³⁶, W. Shaikh¹⁰⁷, A. Shangaraev⁹¹, A. Sharma⁹⁸, A. Sharma⁹⁹, M. Sharma⁹⁹, N. Sharma⁹⁸, A.I. Sheikh¹³⁸, K. Shigaki⁴⁶, M. Shimomura⁸³, S. Shirinkin⁶⁵, Q. Shou^{7,110}, K. Shtejer²⁸, Y. Sibiriak⁸⁸, S. Siddhanta⁵⁵, K.M. Sielewicz³⁶, T. Siemiarczuk⁸⁵, D. Silvermyr⁸¹, G. Simatovic⁹⁰, G. Simonetti^{36,103}, R. Singaraju¹³⁸, R. Singh⁸⁶, R. Singh⁹⁹, V. Singhal¹³⁸, T. Sinha¹⁰⁷, B. Sitar¹⁵, M. Sitta³⁴, T.B. Skaali²³, M. Slupecki¹²⁵, N. Smirnov¹⁴³, R.J.M. Snellings⁶⁴, T.W. Snellman¹²⁵, J. Song²⁰, F. Soramel³¹, S. Sorensen¹²⁷, F. Sozzi¹⁰⁴, I. Sputowska¹¹⁶, J. Stachel¹⁰², I. Stan⁶⁹, P. Stankus⁹⁵, E. Stenlund⁸¹, D. Stocco¹¹², M.M. Storetvedt³⁸, P. Strmen¹⁵, A.A.P. Suaide¹¹⁹, T. Sugitate⁴⁶, C. Suire⁶², M. Suleymanov¹⁶, M. Suljic^{36,27}, R. Sultanov⁶⁵, M. Šumbera⁹⁴, S. Sumowidagdo⁵¹, K. Suzuki¹¹¹, S. Swain⁶⁷, A. Szabo¹⁵, I. Szarka¹⁵, U. Tabassam¹⁶, J. Takahashi¹²⁰, G.J. Tambave²⁴, N. Tanaka¹³⁰, M. Tarhini¹¹², M. Tariq¹⁸, M.G. Tarzila⁴⁸, A. Tauro³⁶, G. Tejada Muñoz², A. Telesca³⁶, C. Terrevoli³¹, B. Teyssier¹³², D. Thakur⁵⁰, S. Thakur¹³⁸, D. Thomas¹¹⁷, F. Thoresen⁸⁹, R. Tieulent¹³², A. Tikhonov⁶³, A.R. Timmins¹²⁴, A. Toia⁷⁰, N. Topilskaya⁶³, M. Toppi⁵², S.R. Torres¹¹⁸, S. Tripathy⁵⁰, S. Trogolo²⁸, G. Trombetta³⁵, L. Tropp⁴⁰, V. Trubnikov³, W.H. Trzaska¹²⁵, T.P. Trzcinski¹³⁹, B.A. Trzeciak⁶⁴, T. Tsuji¹²⁹, A. Tumkin¹⁰⁶, R. Turrisi⁵⁷, T.S. Tveter²³, K. Ullaland²⁴, E.N. Umaka¹²⁴, A. Uras¹³², G.L. Usai²⁶, A. Utrobicic⁹⁷, M. Vala¹¹⁴, J.W. Van Hoorne³⁶, M. van Leeuwen⁶⁴, P. Vande Vyvre³⁶, D. Varga¹⁴², A. Vargas², M. Vargyas¹²⁵, R. Varma⁴⁹, M. Vasileiou⁸⁴, A. Vasiliev⁸⁸, A. Vauthier⁷⁹, O. Vázquez Doce^{103,115}, V. Vechemin¹³⁷, A.M. Veen⁶⁴, E. Vercellin²⁸, S. Vergara Limón², L. Vermunt⁶⁴, R. Vernet⁸, R. Vértesi¹⁴², L. Vickovic³⁷, J. Viinikainen¹²⁵, Z. Vilakazi¹²⁸, O. Villalobos Baillie¹⁰⁸, A. Villatoro Tello², A. Vinogradov⁸⁸, T. Virgili³², V. Vislavicius^{89,81}, A. Vodopyanov⁷⁶, M.A. Völkl¹⁰¹, K. Voloshin⁶⁵, S.A. Voloshin¹⁴⁰, G. Volpe³⁵, B. von Haller³⁶, I. Vorobyev^{115,103}, D. Voscek¹¹⁴, D. Vranic^{104,36}, J. Vrláková⁴⁰, B. Wagner²⁴, H. Wang⁶⁴, M. Wang⁷, Y. Watanabe¹³⁰, M. Weber¹¹¹, S.G. Weber¹⁰⁴, A. Wegrzynek³⁶, D.F. Weiser¹⁰², S.C. Wenzel³⁶, J.P. Wessels¹⁴¹, U. Westerhoff¹⁴¹, A.M. Whitehead¹²³, J. Wiechula⁷⁰, J. Wikne²³, G. Wilk⁸⁵, J. Wilkinson⁵⁴, G.A. Willems^{141,36}, M.C.S. Williams⁵⁴, E. Willsher¹⁰⁸, B. Windelband¹⁰², W.E. Witt¹²⁷, R. Xu⁷, S. Yalcin⁷⁸, K. Yamakawa⁴⁶, S. Yano⁴⁶, Z. Yin⁷, H. Yokoyama^{79,130}, I.-K. Yoo²⁰, J.H. Yoon⁶¹, V. Yurchenko³, V. Zaccolo⁵⁹, A. Zaman¹⁶, C. Zampolli³⁶, H.J.C. Zanoli¹¹⁹, N. Zardoshti¹⁰⁸, A. Zarochentsev¹³⁷, P. Závada⁶⁸, N. Zaviyalov¹⁰⁶, H. Zbroszczyk¹³⁹, M. Zhalov⁹⁶, X. Zhang⁷, Y. Zhang⁷, Z. Zhang^{7,131}, C. Zhao²³, V. Zherebchevskii¹³⁷, N. Zhigareva⁶⁵, D. Zhou⁷, Y. Zhou⁸⁹, Z. Zhou²⁴, H. Zhu⁷, J. Zhu⁷, Y. Zhu⁷, A. Zichichi^{29,11}, M.B. Zimmermann³⁶, G. Zinovjev³, J. Zmeskal¹¹¹, S. Zou⁷,

Affiliation notes

ⁱ Deceased

ⁱⁱ Dipartimento DET del Politecnico di Torino, Turin, Italy

ⁱⁱⁱ M.V. Lomonosov Moscow State University, D.V. Skobeltsyn Institute of Nuclear Physics, Moscow, Russia

^{iv} Department of Applied Physics, Aligarh Muslim University, Aligarh, India

^v Institute of Theoretical Physics, University of Wrocław, Poland

Collaboration Institutes

¹ A.I. Alikhanyan National Science Laboratory (Yerevan Physics Institute) Foundation, Yerevan, Armenia

² Benemérita Universidad Autónoma de Puebla, Puebla, Mexico

³ Bogolyubov Institute for Theoretical Physics, National Academy of Sciences of Ukraine, Kiev, Ukraine

⁴ Bose Institute, Department of Physics and Centre for Astroparticle Physics and Space Science (CAPSS), Kolkata, India

⁵ Budker Institute for Nuclear Physics, Novosibirsk, Russia

⁶ California Polytechnic State University, San Luis Obispo, California, United States

⁷ Central China Normal University, Wuhan, China

⁸ Centre de Calcul de l'IN2P3, Villeurbanne, Lyon, France

- ⁹ Centro de Aplicaciones Tecnológicas y Desarrollo Nuclear (CEADEN), Havana, Cuba
- ¹⁰ Centro de Investigación y de Estudios Avanzados (CINVESTAV), Mexico City and Mérida, Mexico
- ¹¹ Centro Fermi - Museo Storico della Fisica e Centro Studi e Ricerche “Enrico Fermi”, Rome, Italy
- ¹² Chicago State University, Chicago, Illinois, United States
- ¹³ China Institute of Atomic Energy, Beijing, China
- ¹⁴ Chonbuk National University, Jeonju, Republic of Korea
- ¹⁵ Comenius University Bratislava, Faculty of Mathematics, Physics and Informatics, Bratislava, Slovakia
- ¹⁶ COMSATS Institute of Information Technology (CIIT), Islamabad, Pakistan
- ¹⁷ Creighton University, Omaha, Nebraska, United States
- ¹⁸ Department of Physics, Aligarh Muslim University, Aligarh, India
- ¹⁹ Department of Physics, Ohio State University, Columbus, Ohio, United States
- ²⁰ Department of Physics, Pusan National University, Pusan, Republic of Korea
- ²¹ Department of Physics, Sejong University, Seoul, Republic of Korea
- ²² Department of Physics, University of California, Berkeley, California, United States
- ²³ Department of Physics, University of Oslo, Oslo, Norway
- ²⁴ Department of Physics and Technology, University of Bergen, Bergen, Norway
- ²⁵ Dipartimento di Fisica dell’Università ‘La Sapienza’ and Sezione INFN, Rome, Italy
- ²⁶ Dipartimento di Fisica dell’Università and Sezione INFN, Cagliari, Italy
- ²⁷ Dipartimento di Fisica dell’Università and Sezione INFN, Trieste, Italy
- ²⁸ Dipartimento di Fisica dell’Università and Sezione INFN, Turin, Italy
- ²⁹ Dipartimento di Fisica e Astronomia dell’Università and Sezione INFN, Bologna, Italy
- ³⁰ Dipartimento di Fisica e Astronomia dell’Università and Sezione INFN, Catania, Italy
- ³¹ Dipartimento di Fisica e Astronomia dell’Università and Sezione INFN, Padova, Italy
- ³² Dipartimento di Fisica ‘E.R. Caianiello’ dell’Università and Gruppo Collegato INFN, Salerno, Italy
- ³³ Dipartimento DISAT del Politecnico and Sezione INFN, Turin, Italy
- ³⁴ Dipartimento di Scienze e Innovazione Tecnologica dell’Università del Piemonte Orientale and INFN Sezione di Torino, Alessandria, Italy
- ³⁵ Dipartimento Interateneo di Fisica ‘M. Merlin’ and Sezione INFN, Bari, Italy
- ³⁶ European Organization for Nuclear Research (CERN), Geneva, Switzerland
- ³⁷ Faculty of Electrical Engineering, Mechanical Engineering and Naval Architecture, University of Split, Split, Croatia
- ³⁸ Faculty of Engineering and Science, Western Norway University of Applied Sciences, Bergen, Norway
- ³⁹ Faculty of Nuclear Sciences and Physical Engineering, Czech Technical University in Prague, Prague, Czech Republic
- ⁴⁰ Faculty of Science, P.J. Šafárik University, Košice, Slovakia
- ⁴¹ Frankfurt Institute for Advanced Studies, Johann Wolfgang Goethe-Universität Frankfurt, Frankfurt, Germany
- ⁴² Gangneung-Wonju National University, Gangneung, Republic of Korea
- ⁴³ Gauhati University, Department of Physics, Guwahati, India
- ⁴⁴ Helmholtz-Institut für Strahlen- und Kernphysik, Rheinische Friedrich-Wilhelms-Universität Bonn, Bonn, Germany
- ⁴⁵ Helsinki Institute of Physics (HIP), Helsinki, Finland
- ⁴⁶ Hiroshima University, Hiroshima, Japan
- ⁴⁷ Hochschule Worms, Zentrum für Technologietransfer und Telekommunikation (ZTT), Worms, Germany
- ⁴⁸ Horia Hulubei National Institute of Physics and Nuclear Engineering, Bucharest, Romania
- ⁴⁹ Indian Institute of Technology Bombay (IIT), Mumbai, India
- ⁵⁰ Indian Institute of Technology Indore, Indore, India
- ⁵¹ Indonesian Institute of Sciences, Jakarta, Indonesia
- ⁵² INFN, Laboratori Nazionali di Frascati, Frascati, Italy
- ⁵³ INFN, Sezione di Bari, Bari, Italy
- ⁵⁴ INFN, Sezione di Bologna, Bologna, Italy
- ⁵⁵ INFN, Sezione di Cagliari, Cagliari, Italy
- ⁵⁶ INFN, Sezione di Catania, Catania, Italy
- ⁵⁷ INFN, Sezione di Padova, Padova, Italy
- ⁵⁸ INFN, Sezione di Roma, Rome, Italy
- ⁵⁹ INFN, Sezione di Torino, Turin, Italy

- 60 INFN, Sezione di Trieste, Trieste, Italy
- 61 Inha University, Incheon, Republic of Korea
- 62 Institut de Physique Nucléaire d’Orsay (IPNO), Institut National de Physique Nucléaire et de Physique des Particules (IN2P3/CNRS), Université de Paris-Sud, Université Paris-Saclay, Orsay, France
- 63 Institute for Nuclear Research, Academy of Sciences, Moscow, Russia
- 64 Institute for Subatomic Physics, Utrecht University/Nikhef, Utrecht, Netherlands
- 65 Institute for Theoretical and Experimental Physics, Moscow, Russia
- 66 Institute of Experimental Physics, Slovak Academy of Sciences, Košice, Slovakia
- 67 Institute of Physics, Bhubaneswar, India
- 68 Institute of Physics of the Czech Academy of Sciences, Prague, Czech Republic
- 69 Institute of Space Science (ISS), Bucharest, Romania
- 70 Institut für Kernphysik, Johann Wolfgang Goethe-Universität Frankfurt, Frankfurt, Germany
- 71 Instituto de Ciencias Nucleares, Universidad Nacional Autónoma de México, Mexico City, Mexico
- 72 Instituto de Física, Universidade Federal do Rio Grande do Sul (UFRGS), Porto Alegre, Brazil
- 73 Instituto de Física, Universidad Nacional Autónoma de México, Mexico City, Mexico
- 74 iThemba LABS, National Research Foundation, Somerset West, South Africa
- 75 Johann-Wolfgang-Goethe Universität Frankfurt Institut für Informatik, Fachbereich Informatik und Mathematik, Frankfurt, Germany
- 76 Joint Institute for Nuclear Research (JINR), Dubna, Russia
- 77 Korea Institute of Science and Technology Information, Daejeon, Republic of Korea
- 78 KTO Karatay University, Konya, Turkey
- 79 Laboratoire de Physique Subatomique et de Cosmologie, Université Grenoble-Alpes, CNRS-IN2P3, Grenoble, France
- 80 Lawrence Berkeley National Laboratory, Berkeley, California, United States
- 81 Lund University Department of Physics, Division of Particle Physics, Lund, Sweden
- 82 Nagasaki Institute of Applied Science, Nagasaki, Japan
- 83 Nara Women’s University (NWU), Nara, Japan
- 84 National and Kapodistrian University of Athens, School of Science, Department of Physics, Athens, Greece
- 85 National Centre for Nuclear Research, Warsaw, Poland
- 86 National Institute of Science Education and Research, HBNI, Jatni, India
- 87 National Nuclear Research Center, Baku, Azerbaijan
- 88 National Research Centre Kurchatov Institute, Moscow, Russia
- 89 Niels Bohr Institute, University of Copenhagen, Copenhagen, Denmark
- 90 Nikhef, National institute for subatomic physics, Amsterdam, Netherlands
- 91 NRC Kurchatov Institute IHEP, Protvino, Russia
- 92 NRNU Moscow Engineering Physics Institute, Moscow, Russia
- 93 Nuclear Physics Group, STFC Daresbury Laboratory, Daresbury, United Kingdom
- 94 Nuclear Physics Institute of the Czech Academy of Sciences, Řež u Prahy, Czech Republic
- 95 Oak Ridge National Laboratory, Oak Ridge, Tennessee, United States
- 96 Petersburg Nuclear Physics Institute, Gatchina, Russia
- 97 Physics department, Faculty of science, University of Zagreb, Zagreb, Croatia
- 98 Physics Department, Panjab University, Chandigarh, India
- 99 Physics Department, University of Jammu, Jammu, India
- 100 Physics Department, University of Rajasthan, Jaipur, India
- 101 Physikalisches Institut, Eberhard-Karls-Universität Tübingen, Tübingen, Germany
- 102 Physikalisches Institut, Ruprecht-Karls-Universität Heidelberg, Heidelberg, Germany
- 103 Physik Department, Technische Universität München, Munich, Germany
- 104 Research Division and ExtreMe Matter Institute EMMI, GSI Helmholtzzentrum für Schwerionenforschung GmbH, Darmstadt, Germany
- 105 Rudjer Bošković Institute, Zagreb, Croatia
- 106 Russian Federal Nuclear Center (VNIIEF), Sarov, Russia
- 107 Saha Institute of Nuclear Physics, Kolkata, India
- 108 School of Physics and Astronomy, University of Birmingham, Birmingham, United Kingdom
- 109 Sección Física, Departamento de Ciencias, Pontificia Universidad Católica del Perú, Lima, Peru
- 110 Shanghai Institute of Applied Physics, Shanghai, China

- 111 Stefan Meyer Institut für Subatomare Physik (SMI), Vienna, Austria
- 112 SUBATECH, IMT Atlantique, Université de Nantes, CNRS-IN2P3, Nantes, France
- 113 Suranaree University of Technology, Nakhon Ratchasima, Thailand
- 114 Technical University of Košice, Košice, Slovakia
- 115 Technische Universität München, Excellence Cluster 'Universe', Munich, Germany
- 116 The Henryk Niewodniczanski Institute of Nuclear Physics, Polish Academy of Sciences, Cracow, Poland
- 117 The University of Texas at Austin, Austin, Texas, United States
- 118 Universidad Autónoma de Sinaloa, Culiacán, Mexico
- 119 Universidade de São Paulo (USP), São Paulo, Brazil
- 120 Universidade Estadual de Campinas (UNICAMP), Campinas, Brazil
- 121 Universidade Federal do ABC, Santo Andre, Brazil
- 122 University College of Southeast Norway, Tonsberg, Norway
- 123 University of Cape Town, Cape Town, South Africa
- 124 University of Houston, Houston, Texas, United States
- 125 University of Jyväskylä, Jyväskylä, Finland
- 126 University of Liverpool, Department of Physics Oliver Lodge Laboratory, Liverpool, United Kingdom
- 127 University of Tennessee, Knoxville, Tennessee, United States
- 128 University of the Witwatersrand, Johannesburg, South Africa
- 129 University of Tokyo, Tokyo, Japan
- 130 University of Tsukuba, Tsukuba, Japan
- 131 Université Clermont Auvergne, CNRS/IN2P3, LPC, Clermont-Ferrand, France
- 132 Université de Lyon, Université Lyon 1, CNRS/IN2P3, IPN-Lyon, Villeurbanne, Lyon, France
- 133 Université de Strasbourg, CNRS, IPHC UMR 7178, F-67000 Strasbourg, France, Strasbourg, France
- 134 Université Paris-Saclay Centre d'Études de Saclay (CEA), IRFU, Department de Physique Nucléaire (DPhN), Saclay, France
- 135 Università degli Studi di Pavia, Pavia, Italy
- 136 Università di Brescia, Brescia, Italy
- 137 V. Fock Institute for Physics, St. Petersburg State University, St. Petersburg, Russia
- 138 Variable Energy Cyclotron Centre, Kolkata, India
- 139 Warsaw University of Technology, Warsaw, Poland
- 140 Wayne State University, Detroit, Michigan, United States
- 141 Westfälische Wilhelms-Universität Münster, Institut für Kernphysik, Münster, Germany
- 142 Wigner Research Centre for Physics, Hungarian Academy of Sciences, Budapest, Hungary
- 143 Yale University, New Haven, Connecticut, United States
- 144 Yonsei University, Seoul, Republic of Korea